DOI: 10.1002/anie.200906010

Multicomponent Nanoparticles

Colloidal Hybrid Nanostructures: A New Type of Functional Materials

*Ronny Costi, Aaron E. Saunders, and Uri Banin**

Keywords:
heterogeneous catalysis · metals · nanocrystals · semiconductors · shape control

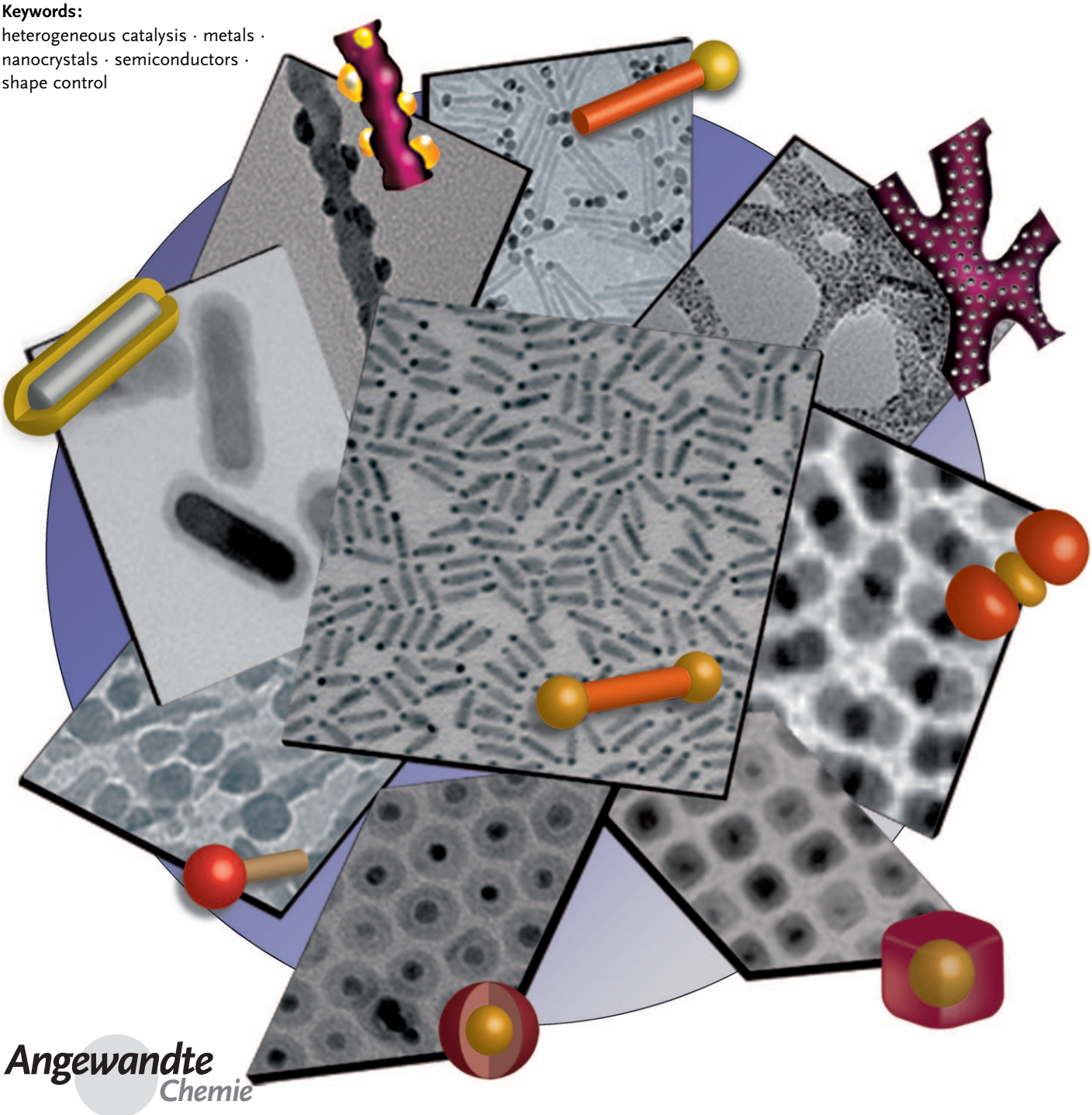

Angewandte International Edition Chemie

One key goal of nanocrystal research is the development of experimental methods to selectively control the composition and shape of nanocrystals over a wide range of material combinations. The ability to selectively arrange nanosized domains of metallic, semiconducting, and magnetic materials into a single hybrid nanoparticle offers an intriguing route to engineer nanomaterials with multiple functionalities or the enhanced properties of one domain. In this Review, we focus on recent strategies used to create semiconductor–metal hybrid nanoparticles, present the emergent properties of these multicomponent materials, and discuss their potential applicability in different technologies.

From the Contents

1. Introduction

Colloidal nanocrystals are mesoscopic materials occupying the region between the atomistic and the macroscopic worlds.[1,2] The physical properties of these tiny crystals of metals or semiconductors manifest the transition from molecular limit to the solid state providing benchmark systems for experimental and theoretical studies of size effects.[3,4] In recent years, there have been tremendous developments in the synthetic control of nanocrystal size, shape, and composition, thus allowing the tailoring of their properties.[5–8] These properties, alongside with the ability to manipulate them using the powerful tools of wet chemistry, also leads to potential applications of colloidal nanocrystals in diverse fields, such as biological tagging,[9,10] medical diagnostics and treatment,[11,12] optical and electro-optical applications,[13–15] solar energy harvesting,[16,17] and more.[18]

In a macroscopic structure, different materials are integrated together to provide the system with tailored properties from the disparate components. For example, metallic contacts are integrated on a semiconductor device by employing highly advanced top-down fabrication methods. In such systems, each component usually retains its original properties while modifications are confined to the interfacial region, which is much smaller than the entire system. In nanomaterials, however, new properties can be attained by combining several materials on the same nanosystem, where due to the small size, the effect of synergetic properties of the separate components may become a dominant factor. For instance, the challenge of contacting small nanocrystals to an electronic circuit can be addressed by growing metallic nanoparticle (NP) contacts onto a semiconductor nanocrystal using the bottom-up approach. Such a nanosystem, combining disparate material components, constitutes a hybrid nanoparticle, and provides a powerful strategy for modifying nanoparticle properties. Significant developments have already been made along this path: Figure 1 shows a gallery of hybrid nanoparticles which combine different material systems into the same structure. These hybrids include semiconductor nanorods with metal tips,[19,20] spherical core/shell magnet–semiconductor structures,[21] co-joined sphere–sphere structures[22,23] with metal–metal, metal–magnet, and magnet–semiconductor interfaces, and more.[24–30] In this Review, we focus on recent developments in the research of such systems, with particular focus on hybrid metal–semiconductor nanoparticles.

The successful synthesis of hybrid NPs builds upon the extensive knowledge accumulated on the controlled synthesis of single-component nanocrystals. Significant advances in the understanding of how to control nanocrystal morphology have been made in recent years. This has been achieved by manipulating the reaction chemistry or growth kinetics during synthesis[5,31–34] by using nanocrystal catalysts to promote anisotropic growth,[6,21,35–39] or through the directed attachment of preformed nanocrystals.[40–42] Precise control of shape and size has been achieved for different types of semiconductors. Shape-selective synthesis allows nanometric spheres, rods, tetrapods, tripods, and more elaborate shapes of different semiconductor materials to be produced.[31,43–45] Metal nanoparticles have also been developed extensively. Different shapes of metal nanoparticles have been synthesized, such as spheres and rods.[46–50]

Current experimental studies of ligand-stabilized colloidal nanocrystals and their properties have their roots in the pioneering work by the groups of Brus and of Henglein, who began studying quantum confinement effects in spherical colloidal CdS nanocrystals over two decades ago.[51,52] These early examples of semiconductor nanocrystals were synthesized at room temperature, and although the optical properties showed quantum confinement effects, the size distribution was broad and the particles exhibited only weak luminescence, which was a consequence of crystal defects and poor surface passivation. Bawendi and co-workers later

[*] Dr. R. Costi, Prof. U. Banin
Institute of Chemistry and Center for Nanoscience & Nanotechnology, The Hebrew University
Jerusalem, 91904 (Israel)
Fax: (+972) 2-658-4148
E-mail: banin@chem.ch.huji.ac.il
Homepage: http://chem.ch.huji.ac.il/~nano/
Prof. A. E. Saunders
Department of Chemical & Biological Engineering
The University of Colorado at Boulder
Boulder, CO 80309 (USA)

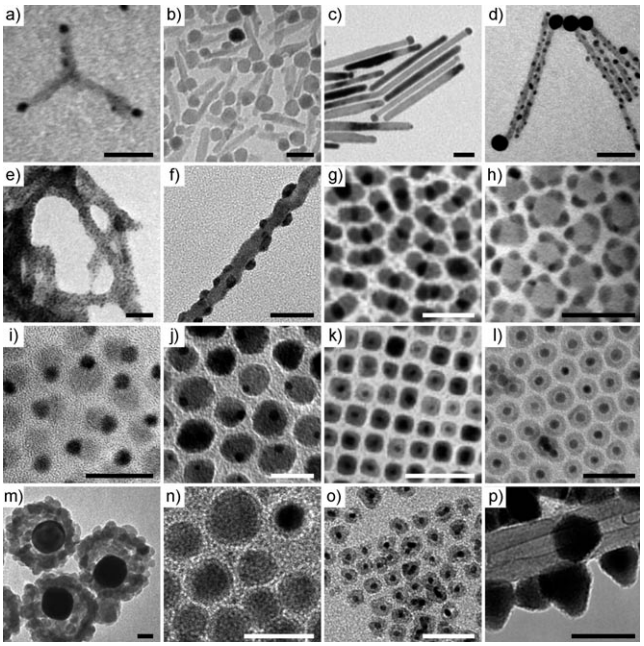

Figure 1. Transmission electron microscopy (TEM) images illustrating the diversity of material combinations and geometries found in hybrid nanomaterials. a) Gold-tipped CdSe nanoparticles; b) Fe_2O_3-tipped TiO_2 nanorods; c) gold-tipped Co nanorods; d) gold-covered CdS nanorods; e) platinum grown onto CdSe networks; f) gold grown onto PbSe nanowires; g) PbS grown onto gold nanocrystals; h) gold grown onto PbS nanocrystals; i) CdS/FePt dimer particles; j) Au/Fe_3O_4 dimer particles; k) Au@Fe_3O_4 particles; l) Au@hollow iron oxide nanocrystals; m) Au@ZnS particles; n) Co@CdSe nanoparticles; o) Pt@hollow Fe_2O_3 nanocrystals; p) CdSe nanocrystals grown onto multiwalled carbon nanotubes. All scale bars: 25 nm. [From: a) Ref. [19], reprinted with permission from the AAAS, b) Ref. [25], copyright 2006 American Chemical Society, c) Ref. [83], d) Ref. [20], copyright 2006 American Chemical Society, e) Ref. [103], f) Ref. [26], copyright 2007 American Chemical Society, g) Ref. [21], copyright 2006 American Chemical Society, h) Ref. [101], copyright 2006 American Chemical Society, i) Ref. [22], copyright 2004 American Chemical Society, j) Ref. [23], copyright 2005 American Chemical Society, k) Ref. [21], copyright 2006 American Chemical Society, l) Ref. [29], m) Ref. [30], n) Ref. [24], copyright 2005 American Chemical Society, o) Ref. [28], copyright 2008 American Chemical Society, p) Ref. [27], copyright 2007 American Chemical Society.]

developed a high-temperature synthesis to decompose organometallic precursors in a coordinating solvent, and produced spherical semiconductor nanocrystals that are monodisperse in size (so-called quantum dots) with greatly improved optical properties.[53] Around the same time, Brust and co-workers developed a two-phase, room-temperature synthetic method for producing small ligand-stabilized gold nanocrystals.[54] Variations on these methods have since been used to synthesize a wide range of semiconducting, metallic, and magnetic nanocrystals.[55]

The bottom-up approach described above has also been successfully extended to shape control, thereby achieving different morphologies. This method proved to be very effective for semiconductor nanocrystals, many of which possess an anisotropic crystal structure that can help drive growth along certain crystal facets, and the presence of an electronic dipole moment that may influence growth. By manipulating the reaction chemistry, Alivisatos, Peng and co-workers first demonstrated the synthesis of CdSe nanorods.[5] This surfactant-controlled growth approach proceeds by the addition of a co-ligand to the reaction mixture that binds preferentially to certain crystal facets, thus favoring growth onto less strongly passivated facets. The anisotropy of the crystals has also been used to synthesize rod-shaped nanocrystals by directed attachment.[56] A highly developed example was provided by Kotov and co-workers, who demonstrated the spontaneous assembly of water-soluble nanocrystals into single-crystal CdTe, Te, and Se nanowires with lengths up to 10 μm and diameters comparable to the original particles (a few nanometers).[40] Partially destabilized nanocrystals were used in which dipole–dipole interactions along the *c* axis of the hexagonal crystal induced registry in the particle orientations while fusing occurred. Similar results for PbSe nanocrystals with a cubic crystal structure have also been shown, resulting in the formation of high-aspect-ratio nanowires with tunable diameters, nanorings, branched structures, and multi-arm (star-shaped) particles.[41,42] These impressive assembled structures are the result of two factors: a) dipole moments can exist along different crystallographic axes in the cubic crystal structure system, allowing bending and corners to be introduced into the growing structures, and b) the use of multiple surfactants during synthesis to further direct the growth process. Another strategy that was applied for the shape control of cubic semiconductor nanocrystals was the use of metal seed to catalyze the growth of colloidal

Ronny Costi received his B.Sc. in chemistry in 2003 and his Ph.D. in 2010 from the Hebrew University of Jerusalem, where he worked with Prof. Uri Banin. His Ph.D. research focused on light-induced processes in hybrid metal–semiconductor nanoparticles. He is currently a postdoctoral researcher with Prof. Daniel G. Nocera at the Massachusetts Institute of Technology.

Aaron E. Saunders received his BS from Iowa State University in 2001, and completed his Ph.D. with Prof. Brian Korgel at the University of Texas at Austin in 2005. He was a postdoctoral researcher with Prof. Uri Banin, studying the synthesis and properties of metal–semiconductor hybrid nanocrystals. He is currently an assistant professor at the University of Colorado at Boulder, researching the synthesis and application of metal chalcogenide nanocrystals for thermoelectric and photovoltaic devices.

nanorods and nanowires by the solution–liquid–solid growth mechanism.[6,57,58]

Shape-control strategies also allowed the preparation of colloidal metal nanorods and nanowires. An example is the seed-mediated growth method used to make gold and silver nanorods and nanowires with controllable aspect ratios.[59] The basic approach employed faceted seed nanoparticles capped by a variety of surface groups (such as citrate surfactants) that were prepared from metal salts using a strong reducing agent. Different solutions containing structure-directing surfactants along with a weak reducing agent were then used sequentially to direct the growth of metal on the seeds. The method is based on the concept that the weak reducing agent can only actively lead to metal growth in the presence of the seed. Electrochemical approaches were also used to prepare metal nanorods and nanowires, especially for noble metals.[60–62] Other work has demonstrated the ability to control metal nanoparticle shapes by exploiting the anisotropy of crystal facets and employing different surfactants.[8]

These extensive synthetic developments of single component colloidal nanocrystals allowed detailed studies of their size and shape dependent properties to be conducted in parallel. As the wavefunctions of electrons and holes are confined by the physical nanometric dimensions of the nanocrystals, the electronic level structure and the resultant optical and electrical properties are greatly modified. Upon reducing the size of direct-gap semiconductors into the nanocrystal regime, a characteristic blue shift of the band gap appears. A discrete level structure develops as a result of the quantum confinement effect,[63] which can be readily observed in the absorption and luminescence spectra of colloidal quantum dots. Furthermore, because of their small size, the charging energy associated with addition or removal of a single electron is very high, leading to pronounced single electron tunneling effects as measured in scanning tunneling spectroscopy studies.[64–66] Metal nanoparticles also exhibit size-dependent properties in which the conduction electron cloud can be driven by an electromagnetic field, producing a resonant surface-plasmon response. For metals with free electrons, the surface plasmon resonance appears in the visible range, leading to vivid color changes of colloidal solutions of nanoparticles of different sizes.[67]

Shape modification also dictates function for both semiconductor and metal nanoparticles. While the emission of spherical semiconductor quantum dots is typically non-polarized, quantum rods show a polarized emission, which also leads to polarized lasing.[15,68,69] For metals, different shapes modify the particle plasmon response. For example, in the case of metal rods, two plasmon resonances can be observed, one at shorter wavelength related to the diameter, and a second, related to the long axis of the rod.[70–73]

An additional way to further enrich the properties of colloidal nanocrystals has been the preparation of heterostructures in which materials of similar type (such as two or more semiconductors) are combined on one nanocrystal. For colloidal semiconductor heterostructures, the prevailing approach consists of growing a few monolayers of a second semiconductor material on top of the core nanocrystal. Within this family of core/shell nanocrystals, a particularly useful combination has been the case where the shell material has a wider bandgap enclosing that of the core (type I band offset). In such a case the exciton is spatially confined to the core, lowering the non-radiative decay through trapping of charge in surface defects, thus resulting in significantly increased quantum yield and photochemical stability.[74–76] If the band gap of the shell forms a staggered offset with the core band gap (a type II offset), one carrier will be confined to the core material and the second carrier will transfer into the shell material.[34,77–81] In such materials, exciton recombination typically occurs across the material interface, and the resulting emission has a lower energy than would be possible using either the core or shell material alone. This effect opens the possibility of using materials that would normally emit in the visible wavelengths for applications requiring near-infrared emission. Although such heterostructures are not the focus of this Review, they demonstrate the possibilities available for enriching nanocrystal function by the combination of several materials on one nanostructure. In metal nanocrystals, binary metallic particles also provide enhanced properties in both magnetic and catalytic functions.[82–84]

The combination of highly evolved synthetic control, along with the fundamental understanding of size- and shape-dependent properties of single-material nanocrystals, has already opened up several directions of application of colloidal nanocrystals in diverse fields. Nanoparticles are used in biology and medicine as tagging agents.[9,10] Semiconductor nanocrystals are emerging as a new class of fluorescent tags by exploiting their tunable optical properties and the ability to manipulate them chemically. Magnetic nanoparticles are being developed as contrast agents for magnetic resonance imaging (MRI).[11,85,86] Optical devices, such as laser gain media and light-emitting diodes, have been demonstrated using colloidal semiconductor nanocrystals of various types.[13–15] Nanocrystal-based field-effect transistors are also of interest for electronic applications.[18] In photovoltaic applications, incorporation of semiconductor nanocrystals as sensitizers and components of solar cells is also under extensive study, in which the potentially scalable and cost-effective wet-chemical processing is of significant advantage.[16,17,87,88] The large surface-to-weight ratio inherent in nanocrystals has also impacted their utilization in heterogeneous catalysis. Here, size effects in metal nanocrystals

Uri Banin received his Ph.D. on femtochemistry in 1994 from the Hebrew University of Jerusalem. During his postdoctoral studies at the University of California at Berkeley (1994–97) he became fascinated by the chemistry and physics of semiconductor nanocrystals. He is a Professor of Chemistry and the Director of the Kreuger Family Center for Nanoscience and Nanotechnology at the Hebrew University of Jerusalem. His research interests focus on the chemistry and physics of nanocrystals (synthesis of novel nanoparticles, studies of size- and shape-dependent properties) and on the development of applications for these new materials.

were found to be a critical factor affecting the catalytic activity.[89,90]

These advancements in research and application of single-component nanocrystals set the stage for the present thrust of research on hybrid nanoparticles reviewed herein. Such hybrid nanoparticles, combining disparate materials on one system, present new challenges in synthesis. This stems from the non-trivial chemical and physical interfacing of the different materials in terms of their chemical compatibility, reactivity, and lattice structure. Section 2 will describe the different growth mechanisms discovered to date for hybrid nanoparticles, focusing in particular on metal–semiconductor hybrids. Upon formation of such hybrid nanoparticles, a second challenge arises concerning the understanding of the synergetic properties of the system. The optical and electronic properties of these multifunctional nanostructures often exhibit interesting deviations from their individual components, such as a shift in the plasmon resonance of noble metal nanocrystals or a decrease in the photoluminescence intensity of semiconductor nanocrystals. These changes are attributed to the mutual effects of the electronic properties of the different components, and are discussed in Section 3.

Multicomponent nanostructures show promise for a number of potential uses due to their multiple functionalities. While semiconductor nanomaterials have been suggested as integral components in future-generation electronic devices, their use is often limited by difficulties in forming electrical contacts with neighboring areas. The ability to form integrated metallic contact points within a multicomponent structure is therefore of great value not only for achieving ohmic electrical contacts, but also for utilizing them as anchor points for bottom-up self assembly of the device.

Magnet–semiconductor nanostructures are also of interest; these materials would be very interesting as dual-use biological tags, offering the ability to visualize labeled cells using both magnetic resonance and fluorescence imaging techniques while external magnetic fields may be employed for the directed assembly of such materials.

Another important opportunity for metal–semiconductor hybrid nanoparticles pertains to their use in solar energy harvesting, and in particular in photocatalysis, in which light energy is converted into chemical energy. Here, the semiconductor part of the hybrid can be tailored for optimal light absorption. Combination of the metal part facilitates charge separation, and the reactive metal surface with a large surface area can serve as the proper catalytic substrate for the reactions. These emerging examples will be described in Section 4.

2. Growth Mechanisms of Hybrid Nanoparticles

Synthesis of hybrid nanoparticles requires the combination of two or more dissimilar materials onto one system.[91] This stretches the capabilities of colloidal synthesis, as chemical and structural compatibility between the different components is generally not expected. Moreover, the extensive development of nanocrystal synthesis sets high standards for the products of the reactions both in terms of homogeneity of the nanoparticles and the ability to process them chemically, which requires solubility. Particle crystallinity is also often expected, which is not easy to realize for different material types in light of their diverse crystal structures. Therefore, when examining the synthetic strategies used for hybrid nanoparticles, different growth mechanisms are brought into consideration, which are summarized in Figure 2 and discussed below.

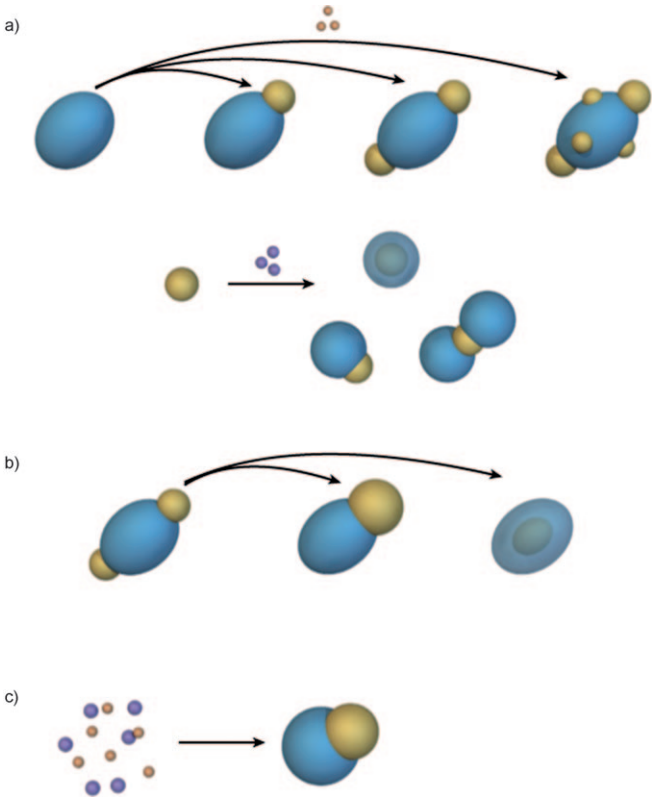

Figure 2. Schemes of growth mechanisms during the synthesis of hybrid nanoparticles. a) Surface nucleation and growth of a second phase on a seed nanoparticle. Top: growth of metal islands on a semiconductor particle; bottom: growth of a semiconductor phase from a metal nanoparticle seed. b) Surface nucleation followed by surface diffusion of the metal phase (middle) or an inward diffusion (right). c) Simultaneous nucleation and growth of both materials.

2.1. Surface Growth

When considering surface growth, the energetics of the reaction plays an important role. The energy barrier for the homogeneous nucleation of a material is typically quite large; it is rare in nanocrystal systems that particles will spontaneously nucleate and grow in solution without a driving force such as a supersaturated solution, a strong reducing agent, or the use of high temperatures to overcome the energy barrier toward nucleation. Attempts to synthesize hybrid nanoparticles make use of this energy barrier, or perhaps more accurately the lower energy barrier for the heterogeneous nucleation of a second phase onto a seed particle (Figure 2a). By understanding the chemistry of the growth process, it is possible to operate in a reaction regime where the heteroge-

neous growth of a second nanocrystal phase is favored over the homogeneous formation of new particles. While the selection of reaction conditions to favor this regime is typically necessary to develop multicomponent nanocrystals, the final structure of the hybrid particles is related to a number of factors, including the size, morphology, and faceting of the nanocrystal seed.

The size of the nanocrystal seed may influence growth in a variety of ways. First, the chemical potential of a nanocrystal surface is inversely related to its radius (the Gibbs–Thompson effect);[92–94] smaller nanocrystals with a high radius of curvature have a higher chemical potential and are expected to be more reactive than larger nanocrystals. Indeed, shell growth in heterostructure semiconductor nanocrystal systems have shown precisely this effect: Dabbousi and co-workers found that the temperature required for the growth of ZnS shells onto CdSe cores increased with increasing core diameter, suggesting that the smaller particles were more reactive.[75] Such results also suggest that for nanocrystal cores with an anisotropic shape, secondary nucleation and growth should occur more rapidly in areas with a high radius of curvature. Similar results have also been observed in the growth of metal islands onto the surface of semiconductor nanorods. While nanorod sides are faceted and relatively flat, the tips are usually much more rounded and should thus exhibit higher surface energy and thus a higher degree of reactivity. Previous work by our group demonstrated that gold nanocrystals preferentially nucleate at the tips of CdSe and CdS nanorods rather than on the sidewalls of the nanorods.[19,20,95,96] Figure 3 demonstrates the selective growth of gold by a simple reaction at room temperature only onto the tips of CdSe nanorods forming "nanodumbbells".

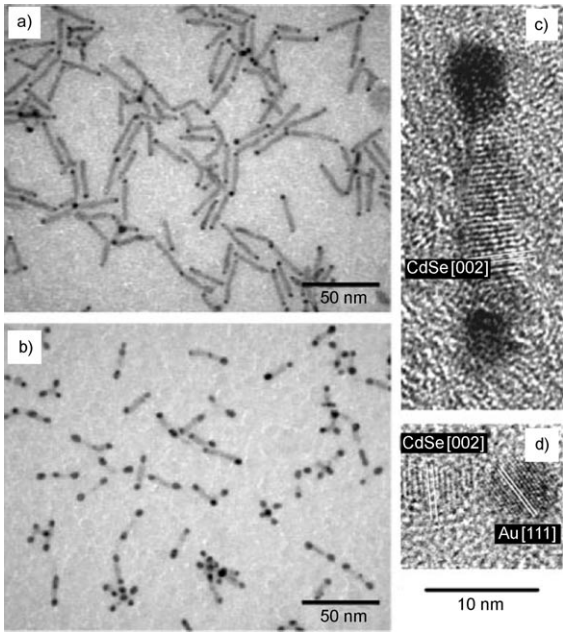

Figure 3. TEM images showing controlled growth of gold onto the tips of CdSe nanorods. a,b) The size of the gold tips can be controlled by varying the amount of gold precursor added during growth. c,d) HRTEM images of a single nanodumbbell (c) and a nanodumbbell tip (d); the CdSe lattice for the rod in the center and gold tips at the rod edges can be identified. [From Ref. [19], reprinted with permission from the AAAS.]

As particle size increases beyond a few nanometers, the appearance of well-defined surface facets may become highly influential in determining where a second phase will nucleate and grow. The presence of facets may allow selective growth to occur due to differences in chemical reactivity, and may be an additional factor contributing to the observed growth behavior for gold onto CdS and CdSe nanorods (Figure 3). The atomic structure of cadmium chalcogenide nanorods is not centrosymmetric; that is, one end facet of the nanorod is typically cadmium-rich, whereas the opposite end is typically chalcogenide-rich.[97,98] The metal–chalcogenide bond enthalpy is typically large, and it is expected that metal nucleation would be easier at such a site. While the growth kinetics in such systems are typically fast and difficult to follow, gold growth onto CdS in the dark occurs relatively slowly at room temperature, and it was observed that gold will nucleate and grow preferentially at a single tip, which was proposed to be the sulfur-rich end, followed by growth onto other sites at longer reactions times.[20] An additional important factor for the selective growth is the ligand coverage of the apex region of the rods relative to the sidewalls. The apexes typically exhibit sparse coverage of ligands, related to the specific facets exposed in the rod ends, which also leads to more reactive surfaces compared with the sidewalls.[99,100]

Another example of facet-controlled growth was demonstrated by Yang and co-workers on a cubic crystal system in which the atomic arrangement in different planes tends to favor additional growth on [111] planes, followed by [110] and [100] sets of planes. In this work, gold and other noble metals were grown onto PbS nanocrystals.[101,102] At low gold concentrations, the gold growth occurred on one spot on the semiconductor core, while at higher concentrations, multiple nucleation sites on the [111] surface facets of the PbS particle took place.

The selective growth onto certain facets or regions of high surface curvature depends on the absence of defects in the original nanocrystal seeds. Defects, whether present during the initial synthesis or introduced through post-processing, provide additional high energy surface sites for nucleation and growth. While gold initially grows onto the tips of CdS nanorods, as mentioned above, further growth was also previously observed onto surface defects as the reaction progressed. The phase transfer of nanocrystal seeds from an organic to water solution may also induce changes at the surface that act as nucleation sites. Figure 4 shows the growth of platinum islands onto the tips and sides of CdSe nanorods following the transfer of the nanorod seeds from an organic to an aqueous phase. Different nanohybrid morphologies were achieved by altering the pH conditions of the growth solution.[103] At high pH, growth of platinum metal on separated CdSe nanorods was observed, whereas at low pH, a CdSe nanonet was formed with platinum metal islands scattered along the nanostructure. This pH dependence was attributed to the dissociation of the mercaptocarboxylic acid ligands from the rod surfaces in acidic conditions, driving fusion of the rods into a nanonet structure.

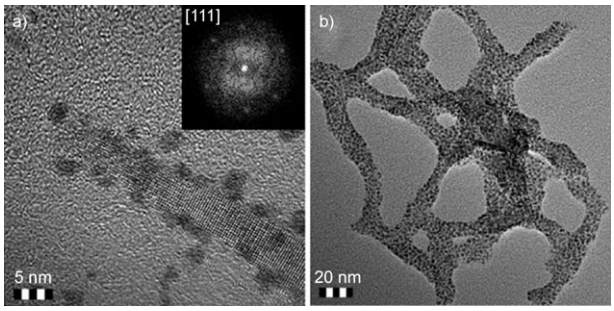

Figure 4. a) HRTEM image of a single CdSe nanorod coated with platinum islands. Inset: Hexagonal spots in the fast Fourier transform (FFT) show the [111] planes of platinum nanocrystals. b) TEM images of CdSe-Pt nanonets. [From Ref. [103].]

Another way to overcome the energetic barrier for metal growth onto a semiconductor nanoparticle is to apply external energy in the form of high temperature or light. Several studies have demonstrated the preparation of hybrid nanoparticles using high temperatures. Casavola and co-workers have demonstrated the high-temperature synthesis of magnetic cobalt metal on oxide semiconductor (TiO_2) nanorods using temperatures exceeding 250 °C.[104] Habas and co-workers have grown Pt, PtCo, and PtNi islands on CdS nanorods at 200 °C.[105] The use of light for metal deposition was also reported. Pacholski and co-workers have demonstrated site-specific photodeposition of single silver nanoparticles on ZnO nanorods;[106] light was used to form single, well-defined metal nanoparticles on the nanorods. Dukovic and co-workers[107] used light for platinum deposition on CdS nanorods and seeded CdSe/CdS nanorods. In the case of CdS nanorods, the light-induced deposition does not show directionality, whereas in the case of CdSe/CdS nanorods, the metal island grows in the vicinity of the CdSe core. Light-induced growth is facilitated by the absorption of above-gap photons by the semiconductor nanoparticle forming electron–hole pairs and thus providing the charge carriers necessary for metal reduction and deposition onto the structure. Often, following the initial nucleation event, the metal island itself serves as the sink for the photoexcited electrons, leading to further metal reduction and growth on the same site. This was observed for light-induced gold deposition onto CdS rods, which resulted in highly selective growth of a large gold tip on one side of the rod.[108,109]

2.2. Surface Growth and Diffusion

Intriguingly, secondary growth mechanisms may occur following an initial surface-growth stage. In some systems, nanocrystals grown at the surface may undergo a diffusion process in which there is a transport process involving the coalescence of surface clusters at a single location, either on the surface of the hybrid particle or within the center of the hybrid particle (Figure 2b). Below we describe two examples: one for each of the above processes.

As described in Section 2.1, the relatively large surface curvature and faceting at the tips of CdSe nanorods leads to selective nucleation and growth of gold in these locations.[19] It was discovered that growth behavior in this material system depends on the concentration of the gold precursor (Figure 5). At low precursor concentration, only surface growth is observed. As the gold precursor concentration is increased, the growth mechanism rapidly undergoes a transition from surface growth to a diffusive process akin to Ostwald ripening.[95] In such growth, one tip is typically slightly larger than the other due to differences in nucleation time or growth rates. During this ripening process, there is a dissolution of the smaller tip while the larger tip grows, which eventually results in disappearance of one tip and growth of the second tip, producing "nano-belltongues" with a gold island at only one tip of the semiconductor nanorod. It is proposed that the process occurs through an Ostwald electrochemical ripening mechanism:[95] as the gold precursor in the solution becomes depleted, the thermodynamically stable size

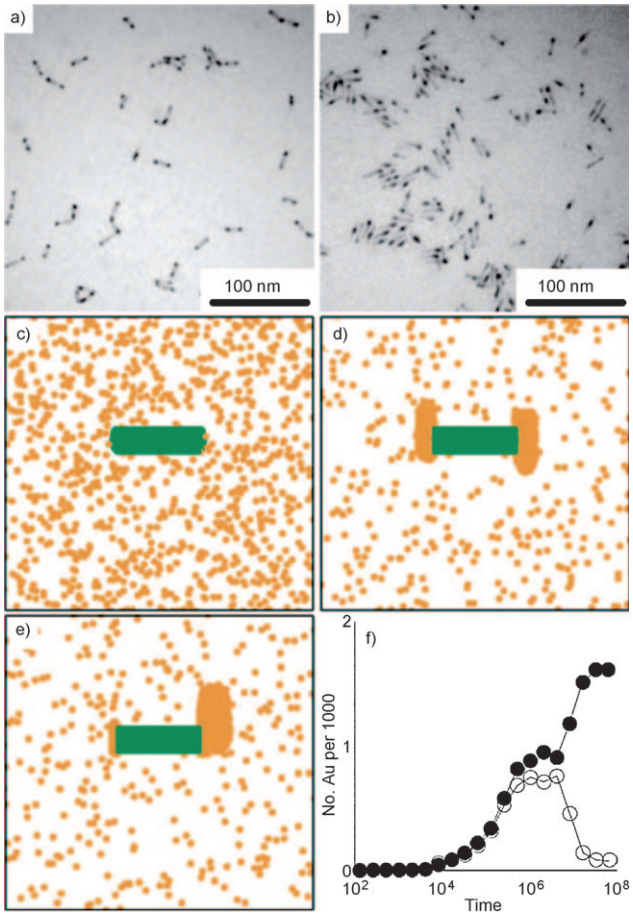

Figure 5. a) Growth of gold onto CdSe nanorods occurs at both tips at low gold precursor concentrations, which is followed by b) a ripening process at high gold precursor concentrations to form one-sided hybrid nanocrystals. c–e) Monte Carlo simulation of the growth dynamics of gold on the nanocrystal: c) Random initial configuration of gold, d) the limit of gold growth onto both tips, and e) the ripening process, in which the larger and more stable right tip continues to grow while at the same time the left tip is nearly fully consumed, to form a one-sided structure. f) Plot of the size of both gold tips showing how they grow together initially, followed by growth of one tip along with a decrease in the size of the other. [From Ref. [95].]

for the gold islands increases. Gold islands smaller than this thermodynamically stable size will dissolve back into the growth medium; as a gold atom is oxidized to become an ion, which can complex with the surfactants in solution, electrons are released into the nanorod. These electrons can then diffuse along the surface of the nanorod to the larger gold particle on the opposite side. The electrons at the second metal tip can then reduce a gold ion from solution, resulting in the overall transport of material from one tip to the other. This transition from surface growth to a ripening behavior has also been observed for gold growth onto CdS nanorods, albeit over much longer timescales (over a period of days for this system, compared with a timescale of minutes for the Au/CdSe system).[20] TEM images for gold growth onto CdSe are shown in Figure 5a,b: the system evolves from gold growth onto both tips at a low concentration of gold salt to a post-ripening system in which the gold has migrated to one tip on each nanorod at a high concentration of gold salt. Snapshots from a Monte Carlo simulation of the growth (Figure 5c–e) show similar effects.[95] A measure of how the size of each gold tip changes during growth is shown in Figure 5f. Initially the growth at each tip is nearly identical; as the gold concentration in the solution is depleted, however, the ripening process leads to the dissolution of one tip while the other increases in size. Selective gold growth onto the seed of CdSe-seeded CdS nanorods with thin shells has also been assigned to such a ripening process.[96] In this case, the CdSe seed serves as a sink for electrons, thus dictating the position for growth of the large gold island.

A different secondary diffusion mechanism has also been observed during the growth of other types of hybrid nanocrystals. The growth of gold onto InAs nanocrystals, for example, also proceeds initially by the formation of gold islands on the surface of the nanocrystal seeds (Figure 6a).[110] These surface islands are not stable over time, and the gold undergoes a secondary diffusion process. In this system, rather than forming a single island on the surface of the particle, the gold atoms diffuse into and coalesce at the center of the InAs nanocrystal, resulting in particles with a core/shell structure (Figure 6b). This process occurs both in solution and in dried films, and therefore does not appear to strongly rely upon changes in chemical potential induced by the precursor concentration, as in the case of Au/CdS and Au/CdSe. One of the factors that appears to influence which diffusion mechanism occurs is the diffusivity of the second component through the first. Solid–solid diffusion coefficients for different systems can vary over many orders of magnitude, so it is not unreasonable to expect that such considerations may help determine the final morphology. At room temperature, the diffusivity $D_{Au/CdS}$ for the Au/CdS system is approximately 10^{-29} $m^2 s^{-1}$.[110] For the Au/InAs system, the diffusion rate is approximately 15 orders of magnitude faster,[110] which would result in diffusion of gold into the semiconductor nanocrystal over much faster timescales, providing qualitative agreement with the observed diffusion behavior in the different systems.

Another elegant diffusion process, leading to hollow nanoparticles, was demonstrated by Alivisatos and co-workers.[111] A Kirkendall effect was used, where the different diffusion rates between two components in a diffusion couple serve to form an empty shell nanoparticle. One example for this process was the formation of hollow CoO nanoparticles from a cobalt sulfide nanoseed, which results from the different diffusion rates of sulfur and oxygen. The approach was further expanded to form hollow nanostructures from oxides, phosphides, and chalcogenides.[112]

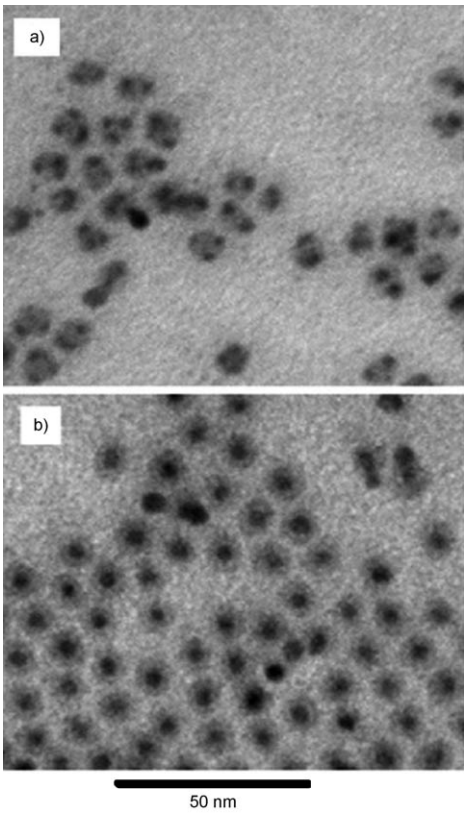

Figure 6. TEM images of InAs nanocrystals after treatment with a gold precursor solution. a) A low gold precursor concentration results in surface growth within two minutes. b) Increasing the precursor concentration by a factor of two results in gold diffusion into the center of the InAs nanocrystals to form a core/shell hybrid nanoparticle. [From Ref. [110].]

At this time it is unclear what the effects of the large surface curvature on these diffusion processes are (for example, the curvature contributes to additional lattice strain within the core particle, which can affect the diffusion process). Further, although gold diffuses into the InAs nanocrystals, which is expected because of the concentration difference between the surface and interior of the particles, this argument would suggest that the gold be distributed homogeneously throughout the InAs nanocrystal; the observed coalescence of the gold particles in the interior is quite unexpected. Additional work is needed to fully explain this behavior and explore other modes of diffusion processes in hybrid nanoparticles.

2.3. Simultaneous Nucleation and Growth of Both Components

The examples in Sections 2.1 and 2.2 involve two distinct processes of nanocrystal nucleation and growth: An initial

process in which nanocrystals are homogeneously nucleated, forming the seed particles, followed by a second process in which another type of material heterogeneously nucleates and grows on the initial seed particle. In some cases, it is possible to use a one-pot synthetic method in which the initial seeds are not isolated before secondary material growth,[22,113] but rather the two components are grown essentially independently. Much rarer are cases in which both components in a hybrid particle nucleate almost simultaneously, followed by growth of each component (Figure 2c). Such behavior has previously been observed for the growth of Ag/AgBr hybrid nanocrystals (Figure 7a,b). Silver ions, which are coordinated

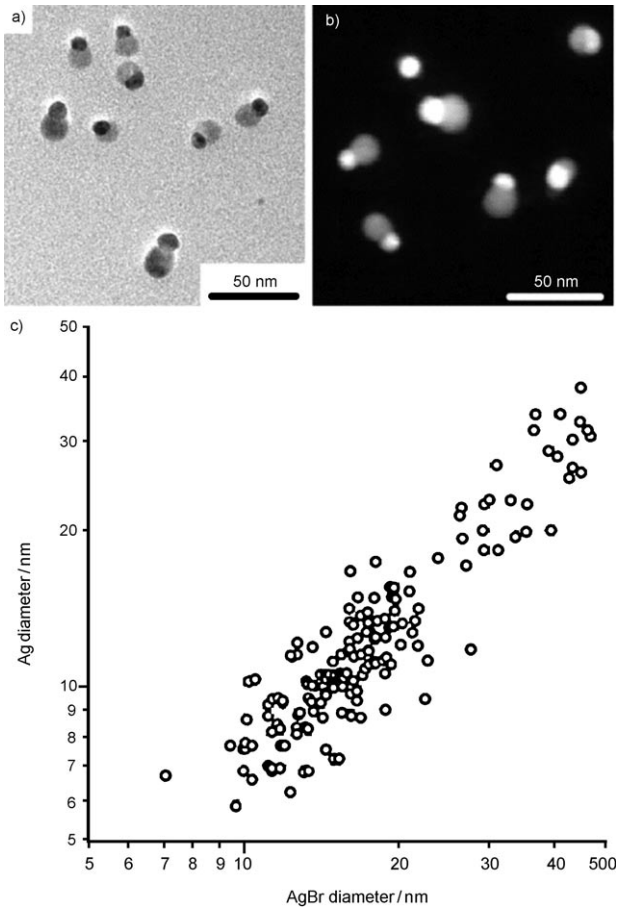

Figure 7. a) TEM and b) STEM images of Ag/AgBr dimer nanocrystals. c) Plot of the respective diameters of each domain of the hybrid nanoparticles, demonstrating a linear relationship over a wide range of sizes. [From Ref. [114].]

to an ionic surfactant containing a bromine counterion, were reduced in the presence of surfactants. The hybrid nanoparticles formed were of a broad size distribution but maintained a well-defined ratio between the sizes of the Ag and AgBr phases (Figure 7c). This suggests that both components nucleate at approximately the same time (Figure 7c), and grow simultaneously.[114] While such systems are interesting to study in terms of particle nucleation and growth kinetics, it is not yet clear whether this type of growth mechanism may be broadly applied to other systems. Furthermore, it is not clear how to separate the nucleation stage from the growth stage, and thus the final size distribution is difficult to control.

2.4. Other Formation Mechanisms

2.4.1. Replacement of a Sacrificial Domain

There have been a few examples of the conversion of heterostructure nanocrystals into hybrid nanoparticles, primarily through the replacement or reaction of a sacrificial component within the heterostructure nanocrystal (Figure 2d). Liu and Guyot-Sionnest reported the synthesis and optical properties of Ag_2S- and Ag_2Se-coated gold nanoparticles.[115] They began by growing gold nanorods and bipyramids in an aqueous phase (Figure 8a), and then grew a

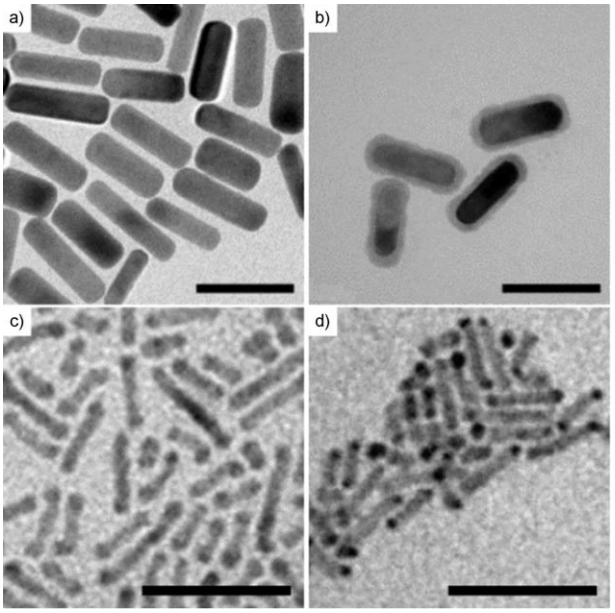

Figure 8. Examples of exchange reactions that result in the formation of hybrid nanoparticles. Gold nanorods (a) are coated with a shell of silver, which is then reacted with selenium to form gold nanorods coated with a Ag_2Se shell (b). CdTe grown at the ends of CdS nanorods (c) is used as a sacrificial template to grow gold tips onto the CdS nanorods (d). Scale bars: 50 nm. [a,b): From Ref. [115], reproduced by permission of the Royal Society of Chemistry, c,d): From Ref. [116], reproduced by permission of the Royal Society of Chemistry.]

conformal layer of silver onto the surface by the heterogeneous reduction of a silver salt at the surface. Sodium sulfide or selenourea was then reacted with the silver coating, resulting in the conversion of the silver layer into a layer of Ag_2S or Ag_2Se, respectively (Figure 8b). The seed geometry and shell thickness could be tuned independently, resulting in hybrid nanocrystals with tunable optical properties.

The synthesis of linear semiconductor heterostructures, in which a second semiconductor is grown only at the tips of a primary semiconductor nanorod core rather than forming a complete shell, have been utilized by Carbone and co-workers

to produce hybrid nanostructures. They found that for certain material combinations, such as CdTe grown onto the tips of CdS nanorods (Figure 8c), the material at the tips could be chemically replaced with gold (Figure 8d).[116] They hypothesize that a redox reaction may be taking place in which gold cations are being reduced as, in this instance, selenium anions are being oxidized. Furthermore, the anions re-dissolve into the surrounding solution. Furthermore, by varying the concentration of surfactants that bind to the gold surface, they were able to destabilize the metal nanocrystals; decreasing the amount of surfactant allowed the gold tips to interact and coalesce, forming disordered networks of fused hybrid nanocrystals. Sacrificial growth was also reported by Sönnichsen and co-workers for hyperbranched CdTe nanostructures. Gold growth on the tips of the CdTe arms was observed.[117] This is an example in which most likely surface growth on the higher energy apexes and sacrificial growth work in tandem to lead to the observed hybrid nanoparticle architecture.

2.4.2. *Self-Assembled Hybrid Nanomaterials*

Although this Review focuses primarily on colloidal metal–semiconductor hybrid nanocparticles, demonstrations of assembled hybrid nanomaterials should also be mentioned. Whereas colloidal hybrid particles consist of two domains physically joined into a single particle, the assembled hybrid materials arise when two colloidal nanoparticle systems with different compositions are brought together via chemical linking agents or by energetics and entropic forces that lead to self-assembly of ordered structures. An example of the former category is work by Kotov and co-workers, who have directed the assembly of streptavadin-coated metal (gold and silver) nanocrystals onto the surface of biotin-coated CdTe nanowires.[118,119] These metal-CdTe hybrid nanomaterials exhibit enhanced photoluminescence, which is due to interactions between the metal nanocrystals and the semiconductor nanowire core.[120]

Within the second category of self-assembling hybrid nanomaterials is work demonstrating the formation of binary nanocrystal superlattices (BNSLs).[121–131] Here, two types of nanocrystals can be deposited simultaneously to form ordered thin films, giving rise to an impressive range of ordered structures that depend primarily on the size ratios and number ratios of the different types of nanocrystals. The formation of these structures is driven by changes in the free volume entropy during drying and by interparticle interactions (notably van der Waals and electrostatic forces). While earlier and ongoing research has focused on the formation mechanisms of these ordered films, there have been a few very recent examples of how the interactions between the nanocrystal components of these films are able to induce changes in properties, such as electron transport or luminescence of the films. Urban and co-workers co-assembled PbTe and Ag_2Te nanocrystals, and found that the presence of the Ag_2Te nanocrystals resulted in a synergistic effect that dramatically increased the p-type conductivity of the films compared with films consisting of only one nanocrystal component or the other.[129] Other work by Shevchenko and co-workers studied the co-assembly of Au and CdSe nanocrystals, and found that BNSLs of this type exhibited reduced fluorescence, which is due to interactions between the metal and semiconducting nanocrystals.[131]

2.5. Structural Characterization of the Interface between Domains

The hybrid nanostructures present a new system with unique interfaces between the different material components. Deciphering the chemical and structural attributes of these metal–semiconductor interfaces is a challenging and ongoing task.

The use of nanocrystals as seed particles has been previously explored, notably in the synthesis of core/shell semiconductor heterostructure nanocrystals. In many of these systems, the semiconductor pairs have similar structural properties, and the interface between the core and shell is nearly epitaxial due to the small mismatch of the lattice distances between the components.[132–134] In fact, many such systems exhibit epitaxial growth of the shell layer, even though the lattice mismatch between materials is larger than what would be allowed in planar systems; it appears that the large radius of curvature at the nanocrystal surface may help to accomodate strain effects that would result in non-epitaxial growth in two-dimensional and bulk interfaces.[75,132,135,136]

Interestingly, although several hybrid nanocrystal systems exhibit epitaxial growth at the interface between the components and the formation of hybrid structures may be enhanced when such growth is possible, it does not appear to be a necessary condition for growth to occur. The latter category, in which growth occurs despite the lack of lattice-matched surface facets, includes the growth of gold onto CdSe and CdS nanorods; a close examination of the interface between CdS and gold domains in this case demonstrated that there was no preferred orientation during growth (Figure 9a).[20] Selection of other material combinations, however, can lead to hybrid nanocrystals that exhibit epitaxial growth of one component onto another. One example is the case of iron oxide nanocrystals grown onto gold seeds to form peanut-like hybrid nanocrystals (Figure 9b).[23] The effect of the degree of mismatch between the crystal lattices of the two components has been studied by Kwon and Shim, who examined the growth of different metal sulfides (ZnS, HgS, and CdS) onto spherical γ-Fe_2O_3 nanocrystals (Figure 9c).[137] Within these systems, the lattice mismatch of the cubic (zinc blende) semiconductors and the iron oxide was 4.0% for ZnS, 4.6% for CdS, and 5.1% for HgS. As the amount of lattice mismatch increased, Kwon and Shim observed fewer instances of junction formation between the semiconductor and magnet domains and an increasing occurrence of homogeneous nucleation of the semiconductor nanocrystals.[137]

3. Optical and Electronic Properties of Hybrid Nanomaterials

The hybrid nanostructures have unique properties, which arise from both the properties of the separate materials in the

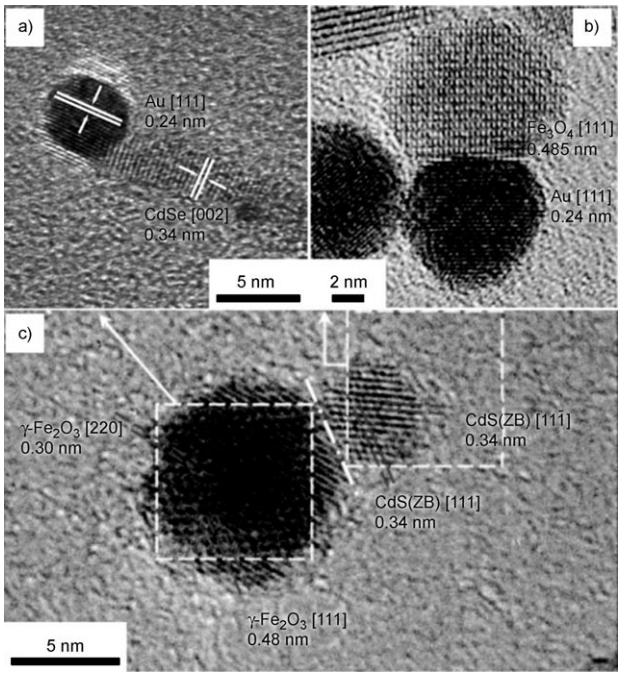

Figure 9. HRTEM images used to characterize the interface between materials in hybrid a) Au-CdSe, b) Au-Fe_3O_4, and c) CdS-Fe_2O_3 nanocrystals. Arrows indicate the measured lattice spacings in the different materials, along with assignments. ZB = zinc blende. There is no epitaxial growth in (a), whereas the systems in both (b) and (c) exhibit epitaxial growth. [a): From Ref. [20], copyright 2006 American Chemical Society, b): From Ref. [23], copyright 2005 American Chemical Society, c): From Ref. [137], copyright 2005 American Chemical Society.]

system as well as from the synergistic properties brought about by the metal–semiconductor contact. Changes in the optical and electronic properties as the result of the combination of multiple materials into a single colloidal particle at the nanoscale may roughly be divided into two categories: a) Multi-functional nanocrystals, in which the composite particles mostly retain the original properties of both materials but are now combined in a single nanoparticle system; and even more interestingly, b) hybrid materials in which the properties of one material show a strong change due to the presence of a second material. The delineation of these two cases is not necessarily straightforward, however. For the same combination of materials, the properties of the resulting hybrid nanomaterial depend not only on the material properties of both components, but also on the morphology of the particle (how each material domain is grown with regard to the other) and how the domains are joined together (whether there is a chemical bond between the materials, or if they are brought together in close proximity using chemical linkers or by self-assembly).

3.1. Optical Properties

Different effects on the optical properties may be expected because of the proximity of semiconductors and metal nanoparticles. Starting with fluorescence, which is a central property of colloidal semiconductor quantum dots, proximity to a metal island leads to interplay between fluorescence quenching[19,103,138] and enhancement effects.[118] Fluorescence quenching may arise from energy transfer from the exciton in the semiconductor to the metal. Enhancement has been observed by Kotov and co-workers by chemically linking gold nanocrystals to the surface of CdTe nanowires. The observed increased quantum yield accompanied by reduced fluorescence lifetime was assigned to the interaction between the collective surface plasmon of the metal nanoparticle and the excitons within the semiconductor nanowire.[118] Using fluorescent dyes tethered to silver nanocrystals, Ginger and co-workers have demonstrated how this type of enhancement depends strongly upon the degree of spectral overlap between the surface plasmon resonance and the fluorescence peak of the dye.[139] Other methods of enhancement are also possible in such systems, such as an increase in the absorption cross-section upon bringing semiconductor and metal regions into close proximity. Generally, such enhancement is often seen in cases in which the semiconducting and metallic domains are separated by a small distance and a large potential barrier is present between the two domains.

An additional important avenue for fluorescence quenching that appears to be dominant in hybrid metal–semiconductor nanoparticles is that of light-induced charge separation at the metal–semiconductor interface. This is most relevant to the case where the two domains are chemically joined, resulting in a direct pathway for charge separation that quenches luminescence. Weller et al. observed the quenching of the luminescence of ZnO nanorods upon the photoreduction of silver domains onto the nanorod surface.[106] We have also observed quenching upon growth of gold domains onto the tips and surface of CdS[20] and CdSe[19] nanorods (Figure 10). Similar quenching effects have also

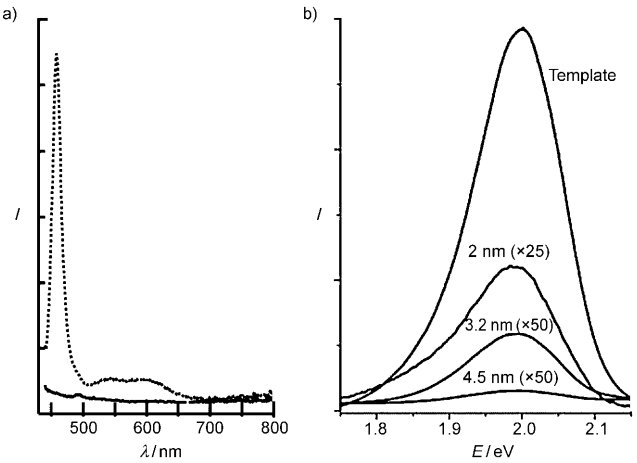

Figure 10. Spectra showing typical photoluminescence quenching that is observed upon growing metal islands onto the surface of semiconductor seed nanocrystals. a) Both the band edge and trap-state emission of CdS nanorods (•••••) is quenched upon the growth of gold (——). b) Similar quenching effects are observed upon the growth of different sizes (2–4.5 nm) of gold tips onto CdSe/ZnS core/shell nanorods (template). [a): From Ref. [20], copyright 2006 American Chemical Society, b): From Ref. [19], reprinted with permission from the AAAS.]

been observed for other geometries and material combinations: Prasad and co-workers studied the growth of Au/PbS and Au/PbSe nanocrystals with dimer, core/shell, and other morphologies,[21,38,140] and Mokari et al. grew gold onto the surface of InAs nanocrystals.[110] The transfer of an electron from CdS, CdSe, or InAs into a gold domain, for example, is facilitated by the presence of the metal Fermi level at an energy within the bandgap of these semiconductors. Upon excitation of an electron into the conduction band of the semiconductor, the electron may then relax into the metal domain, leaving behind the oppositely charged hole and opening rapid nonradiative relaxation pathways.

An intermediate behavior in terms of fluorescence properties was also reported for some metal–semiconductor hybrid nanoparticles. While the growth of gold islands onto the surface of CdS nanorods resulted in quenching, Chen and co-workers grew partial shells of CdS around gold nanocrystal seeds and observed an increase in both the band edge and the trap state luminescence of the semiconductor.[141] This enhancement was attributed to the geometry of the hybrid structure in which energy from the surface plasmon is efficiently transferred to the CdS domain that surrounds the metal core, in contrast to the surface growth of gold onto CdS nanorods, which results in only a limited interface for energy transfer. An alternative explanation is suggested in work by Kim and co-workers, who grew a CdSe shell around metallic cobalt nanocrystal core.[24] They found that the CdSe shell had a low, but not completely quenched, quantum yield. In this instance, however, the semiconductor shell was polycrystalline; the multiple domain walls separating the CdSe crystallites may retard electron transfer to the cobalt core, allowing some radiative exciton recombination to occur.

The absorption of both the semiconducting and metallic domains in hybrid nanoparticles may also exhibit significant changes. Upon growth of metal domains onto a semiconductor nanocrystal, the excitonic features of the semiconductor typically become "washed out", and the excitonic peak and fine structure become much less pronounced. While the overlap of the absorption of both materials is certainly important, the observed absorption spectra of the resulting hybrid structures are typically not linear additions of the absorbance of the individual components.[19–21] Instead, it has been suggested that this is the result of the mixing of the electronic states of the metal and semiconductor,[110] resulting in a modified density of states that affects the absorption spectrum.

During the growth of metal domains onto semiconductor nanocrystal seeds, changes in absorbance appear to be strongly related to the size and number of the metal domains, and may serve as a useful guide to monitor the extent of reaction. These changes are most clearly seen in systems in which the excitonic features are spectrally separated from the plasmonic features of the metal. This is most easily accomplished when using a wide-band-gap semiconductor as the seed, as in the case of silver growth onto ZnO (the silver plasmon occurs at approximately 440 nm, while the ZnO absorption edge occurs near 375 nm),[106] or gold growth onto CdS.[20] Figure 11 shows the change in absorbance of the hybrid nanocrystals in this latter system in comparison to its

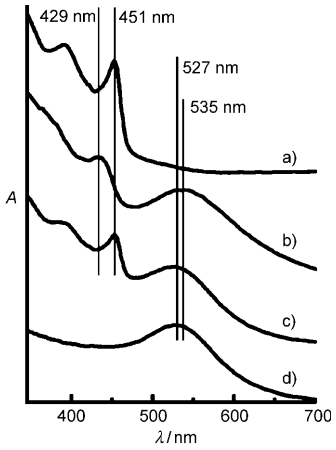

Figure 11. Comparison of the absorption spectra (vertically offset for clarity) of a) free CdS nanorods, b) Au/CdS hybrid nanostructures, c) a physical mixture of free CdS nanorods and gold nanocrystals, and d) free Au nanocrystals. The CdS exciton peak and the gold plasmon peak in the hybrid nanostructures (b) are shifted with respect to the individual components and to the physical mixture of the components. [From Ref. [20], copyright 2006 American Chemical Society.]

separate components and to a mixture of gold nanoparticles and CdS nanorods. The original features of the gold plasmon and the CdS excitonic transition are still discernable in the hybrid nanoparticles. This is expected, as the interface region represents a relatively small fraction of the nanoparticle volume. However, the first exciton transition has clearly shifted to higher energies in the hybrid compared to the CdS rod template and has also broadened slightly. Furthermore, the plasmon peak of the hybrid Au/CdS particles is red-shifted by 8 nm compared with the pure gold nanocrystals, an effect which could be due to the overlap of the electronic states of the different components of the hybrid particles which modifies the surface plasmon resonance. Alternatively, the shift may reflect that the gold portion of the hybrid nanocrystals is partially covered with CdS, which possesses a higher index of refraction than toluene or the organic capping ligands. The presence of a material with a higher index of refraction is expected to shift the gold plasmon toward longer wavelengths, which has been observed experimentally by varying the refractive index of the solvent. For example, Mulvaney and co-workers demonstrated that changing the solvent resulted in a shift of the plasmon peak of gold nanocrystals by up to about 10 nm,[142] which is about the same order of magnitude as the shift of the plasmon in the Au/CdS hybrid nanoparticles. In comparison, the growth of a semiconducting shell of PbS, which has a much larger refractive index than such organic solvents as toluene (approximately 4.3 for PbS compared with about 1.5 for toluene) around a gold core resulted in a shift of the surface plasmon resonance by 50 to 100 nm, depending on the geometry of the hybrid particle.[21]

3.2. Electronic Properties

A fundamental and intriguing problem associated with hybrid nanoparticle systems concerns the electronic properties of the metal–semiconductor nanojunction in such structures. In bulk systems, such an interface is characterized by the space-charge region and the corresponding Schottky barrier.[143] The spatial extent of this interface region is typically tens of nanometers, which is comparable and in many cases larger than the hybrid nanoparticle itself. Therefore, such systems provide the opportunity to re-examine the concepts for the metal–semiconductor interface in nanoscale contacts. From a technological point of view, understanding the properties of such nanocontacts is a major step towards the implementation of semiconductor nanocrystals (as well as molecules) in nanoelectronic device architectures.

The metal–semiconductor nanojunction problem was treated theoretically by Landman and co-workers, who studied the nanocontacts formed between silicon nanowires (a few nanometers long) and aluminum nanoelectrodes. The authors predicted the induction of subgap states near the silicon–aluminum interface, which rapidly decay into the silicon, and the development of relatively large Schottky barriers (Figure 12 I).[144] Experimentally, Steiner and co-workers used scanning tunneling microscopy measurements to probe the electronic band structure at the metal–semiconductor interface of gold-tipped CdSe nanorods.[145] The tunneling spectra (Figure 12 II) show large spatial variations along a single particle. The spectra taken on the gold tips typically portray single-electron tunneling (SET)-like features (namely, the Coulomb blockade and Coulomb staircase), albeit with unequal steps. Spectra measured near the middle of the rod show large energy gaps that are comparable to those observed previously on CdSe rods.[146] A more complex behavior is found near the Au–CdSe interface, where subgap states emerge and then diminish upon moving towards the rod center. This behavior is consistent with the above-mentioned theoretical predictions for the development of metal induced gap states at the interface. These states also lead to a modified Coulomb staircase and in some cases to negative differential conductance on the gold tips.

Another interesting aspect of the nanoscale contact in the hybrid nanoparticles concerns its behavior under illumination. Absorption of above-gap photons by the semiconductor part of the hybrid forms an electron–hole pair. In the case of hybrids of ZnO with different metals, electrons were subsequently transferred into the metal region. The metal region is then charged by the excess electrons, and the charging energy raises its Fermi level until equilibration is reached.[147] Investigations of light-induced charging of hybrid nanoparticles was carried out by electrostatic force microscopy (EFM) on single gold-tipped CdSe nanorods.[148] This method allows the measurement and quantification of charge carriers in single nanoparticles.[149,150] Au/CdSe hybrid nanoparticles exhibit a net negative charging under illumination, while the separate components, gold nanoparticles and CdSe nanorods, exhibit a slight positive charging under illumination. This behavior is attributed to light-induced charge separation that occurs at the metal–semiconductor interface due to the energy band alignment on the nanostructure. After charge separation, the negative charges remain in the metal domains of the hybrid structure while the positive charges are extracted and transferred to the underlying metallic substrate. The light-induced charge separation occurring in hybrid metal–semiconductor nanoparticles is of significant interest for applications in solar energy harvesting and photocatalysis, as discussed in Section 4.2.

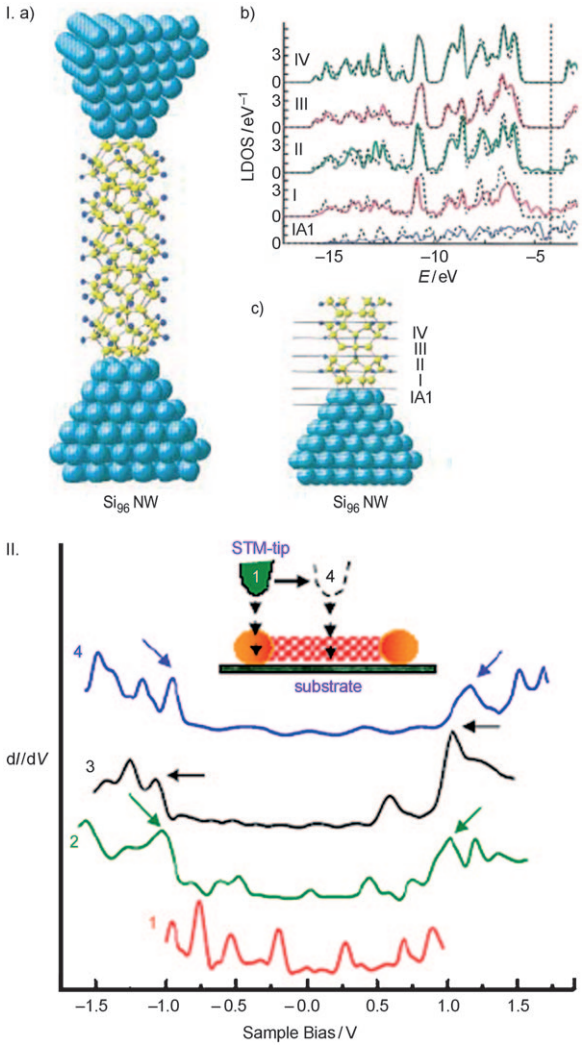

Figure 12. I. a) A model of a silicon nanowire with aluminum tips. b) Local densities of state (LDOS) for undoped Si_{96} nanowire (Si_{96}NW) with aluminum growth. The LDOS is calculated in a cylinder of radius 5.73 Å about the middle axis of the wire, and the various regions are denoted in (c). II. d*I*/d*V* versus voltage spectra measured with scanning tunneling microscopy (STM) on a single Au/CdSe nanodumbbell at different locations. At location 1, above the gold tip position, a modified Coulomb staircase is seen, while in the center of the rod location 4, the band gap of the semiconductor (marked in arrows for graphs 2–4) is seen. Development of states in the bandgap of the semiconductor is seen as the tip approaches the metal–semiconductor interface (spectra 2, 3). The spectra are vertically offset for clarity. [I: From Ref. [144], copyright 2000 American Physical Society, II: From Ref. [145], copyright 2005 American Physical Society.]

Other interesting properties that are of relevance concern the combination of magnetic and semiconductor segments on

the hybrid nanoparticle. For example, cobalt-tipped CdSe nanorods exhibit high-quality magnetic properties that are similar to those of bare cobalt nanocrystals. Moreover, fluorescence of the semiconductor part was also observed, albeit weaker compared to the emission of the original rods.[151] Such combinations are of interest in dual-channel magneto-optical labeling (see Section 4.1.2), and are also potentially of interest in spintronics.

4. Applications of Hybrid Nanocrystals

In addition to fundamental studies of how different material systems combine and interact at the nanoscale, the design aspect of hybrid nanocrystal synthesis is focused on creating multifunctional particles or particles that have new or enhanced properties because of the combination of the properties of each nanoscale component.

4.1. Multifunctional Particles

4.1.1. Anchor Points for Electrical Connections

One potential use for hybrid metal–semiconductor systems involves the growth of metal domains on semiconductor nanomaterials that will serve as integrated electrical contacts to external circuits. A number of strategies have evolved for integrating semiconductor nanorods and nanowires into electrical devices. Typically, nanoscale metal contacts are deposited using electron-beam lithography, focused ion beam (FIB) deposition, or other methods, onto a nanostructure on a substrate.[152,153] However, variation in the contact between the semiconductor nanostructure and the deposited metal films can in some cases lead to irreproducibility, or very high contact resistances. Moreover, such serial high resolution lithographic approaches are demanding and not easily scalable for addressing complex wiring schemes. Metal tips on hybrid nanoparticles may be useful as integrated attachment points to external circuits. The conductance difference present in a metal–semiconductor hybrid nanocrystal is demonstrated in Figure 13, in which gold-tipped CdSe nanorods are characterized using scanning tunneling microscopy (STM; Figure 13a–b)[145] and tunneling atomic force microscopy (tunneling AFM; Figure 13c).[19] The tip region indeed exhibits lower resistance as compared to the rod body; higher tunneling current was observed through the tip, suggesting the tip as a potential electrical contact.

The utility of the metal tips for electrical contacts was directly demonstrated by Sheldon and co-workers, who used a trapping method to localize gold-tipped CdSe nanorods between gold nanoelectrodes.[154] Transport measurements showed that for CdSe nanorods with gold tips grown in solution, the conductance improved remarkably by five orders of magnitude in comparison to CdSe nanorods. This establishes that hybrid nanostructures allow a path for highly improved electrical connectivity of the semiconductor part to the circuit.

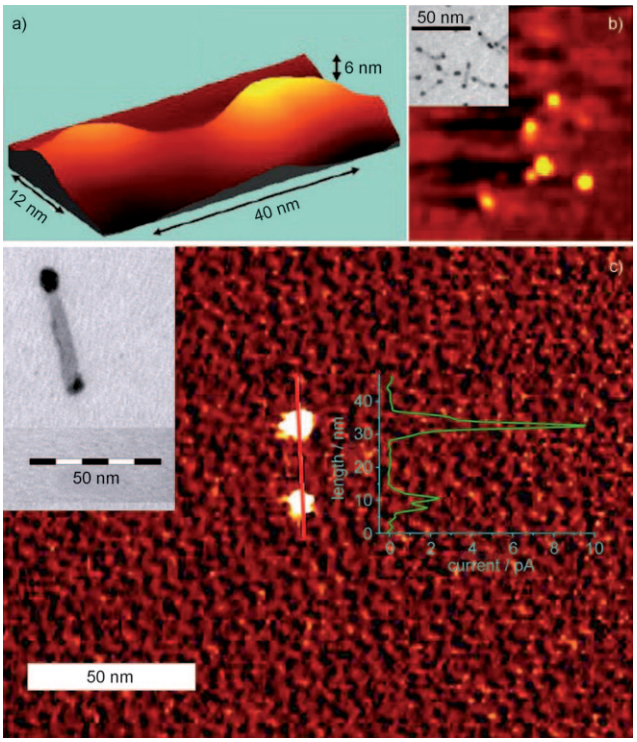

Figure 13. a) Three-dimensional topographical STM image of a single Au/CdSe nanodumbbell. b) Conductance image of the nanodumbbell sample showing high conductance (yellow) through the gold tips; inset: TEM image of the sample. c) A tunneling AFM conductance image of a single nanodumbbell, demonstrating the conductance through the tips; inset: TEM image of a single nanodumbbell. [a,b): From Ref. [145], copyright 2005 American Physical Society, c): From Ref. [19], reprinted with permission from the AAAS.]

4.1.2. Anchor Points for Self-Assembly

Metal tips may also serve as selective sites for the attachment of molecules, allowing the hybrid nanocrystals to be functionalized in specific locations. For example, the bond enthalpy between metals and thiols is typically very high, suggesting that thiolated molecules should show a preferential attachment to the metal parts of the hybrid nanoparticles compared with attachment at other points. This was demonstrated by Salant and co-workers, who attached thiolated biomolecules (disulfide-modified biotin) to metal–semiconductor hybrid nanoparticles and used avidin as a biochemical link between the functionalized particles (Figure 14a).[155] The functionalized hybrid nanoparticles assembled favorably in a tip-to-tip configuration, which was due to the increased binding of the thiolated biotin to the gold tips (Figure 14). Through this strategy, dimer and trimer head-to-tail arrangements could be prepared preferentially. Furthermore, intriguing flower-like structures were observed and attributed to the tetramer binding capability of the central avidin unit. The use of metal tips as anchor points for self-assembly may open a route for parallel bottom-up wiring of vast numbers of hybrid nanoparticles onto electrical devices.

Additional use of metal tips as anchor points for self-assembled structures was demonstrated by Manna and co-workers, who developed a welding mechanism for forming

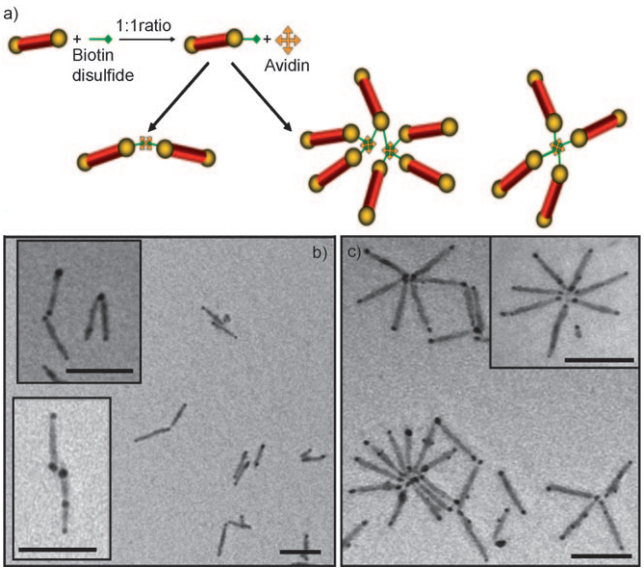

Figure 14. a) Self-assembly of nanodumbbells into dimers and nanoflowers; CdSe red, Au yellow. Nanoflowers are formed due to the tetramer nature of avidin, allowing up to four conjugations of biotin to a single avidin. b,c) TEM images of b) dimers and c) nanoflowers. All scale bars: 50 nm. [From Ref. [155], copyright 2006 American Chemical Society.]

end-to-end structures of gold-tipped semiconductor nanorods. In this procedure, small amounts of I_2 molecules are used to destabilizes the gold nanoparticles and induce coalescence of the gold domains forming complex multiparticle structures.[156] Another work on the self-assembly of gold-tipped semiconductor nanorods was carried out by Kumacheva and co-workers.[157] Here, rods were self-assembled in a stacked vertical configuration (Figure 15). This self-assembly was also achieved by carrying out different surface modifications of the semiconductor and metal parts of the gold-tipped CdSe nanorods. Such vertically assembled structures are of interest for creating contact to a macroscopic array of rods, as they open up a possibility of depositing a top contact electrode. In this context, Ryan and co-workers have demonstrated gold growth on arrays of vertical CdS rods by employing a synthetic approach similar to that used in the solution growth of gold tips.[158]

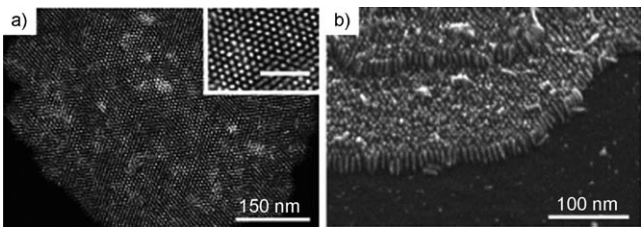

Figure 15. a) Dark-field TEM image of a close-packed self-assembled vertical nanorod array seen from above; inset: magnified view of the array (scale bar: 50 nm). b) SEM image of a side view of the self-assembled array. [From Ref. [157], copyright 2009 American Chemical Society.]

*4.1.3. **Biological and Medical Applications***

A further important direction for applications of hybrid nanoparticles concerns their use as multifunctional biological markers. Considering that semiconductor quantum dots have already emerged as a powerful new family of biological fluorescent tags, and that magnetic nanocrystals are also widely employed as MRI contrast agents, it is clear that combining both functionalities on one hybrid nanoparticle presents a powerful approach with potential implications for medical diagnostics. Ying and co-workers, for example, have synthesized Fe_2O_3/CdSe composite nanocrystals (Figure 16 a–c), which they then coated with a bio-functionalized silica shell to render the nanocrystals biocompatible for labeling experiments of live cell membranes (Figure 16 d,e).[159] The composite particles can be recovered using magnetic filtration, and were shown to target cell membranes for use in fluorescence imaging. This combination of properties suggests

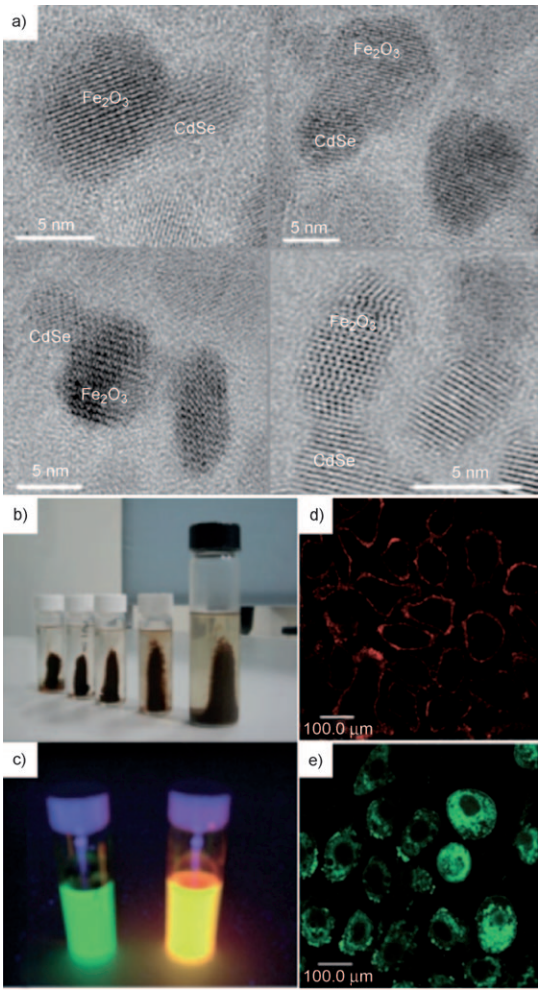

Figure 16. a) TEM images of hybrid CdSe/Fe_2O_3 nanocrystals, b) their magnetic properties, using a magnetic field to harvest them from solution, and c) luminescent properties. d,e) Confocal laser scanning microscopy images demonstrating the use of these silica-coated hybrid nanocrystals for fluorescent labeling of live cell membranes. [From Ref. [159].]

applicability for simultaneous imaging and magnetic-field-directed movement of individual cells.

Other combinations of materials may also be of future interest in biological applications. The synthesis of composite magnet–noble metal hybrid nanocrystals, which retain both plasmonic features and a strong response to magnetic fields, has been reported.[160] Here, scattering of the plasmon alongside with magnetic contrast may be envisioned.

4.2. Enhanced Functionality: Photocatalysis and Solar Energy Applications

Another strategy in the design of hybrid nanostructures is to combine materials so as to increase the functionality of one of the components by synergy between the different materials. To date, the most widely studied application in this regard is the enhanced photocatalytic activity of semiconductor nanoparticles upon combination with metals. Photocatalysis with semiconductors has been studied extensively because of its potential in environmental applications[161,162] such as photodegradation of organic contaminants for water purification, and in energy applications such as photoelectrochemical cells,[163] and hydrogen generation by water splitting.[164–168] Early studies focused mostly on wide-gap metal oxide nanocrystals, demonstrating important design parameters in single-component systems.[169–172] Following light absorption, a competing mechanism with photocatalysis is the recombination of the electron–hole pair. Growth of a metal island, leading to charge separation, can suppress the undesired recombination process; furthermore, it provides catalytic surface with a large area for the ensuing redox reactions.

For metal–semiconductor hybrid nanoarticles, photon absorption into the semiconductor region generates an electron–hole pair, followed by the fast transfer of one of the charge carriers into the closely spaced energy levels in the metal domains (Figure 17). While this charge separation results in quenching of the photoluminescence (as discussed in Section 3.1.1), the separated charge carriers may be used in redox reactions. Work by Kamat and co-workers on silver nanocrystals covered by TiO_2 nanoclusters[173–175] has demonstrated that, upon absorption of UV light by TiO_2, and with the solvent acting as a hole acceptor, electrons are efficiently stored in the metal. This effect was inferred from a pronounced shift in the location of the silver plasmon absorption. When electron acceptor molecules are present in solution, the photogenerated charge carriers can contribute to redox reactions, as shown in the reduction of thionine dye in Figure 18.[173]

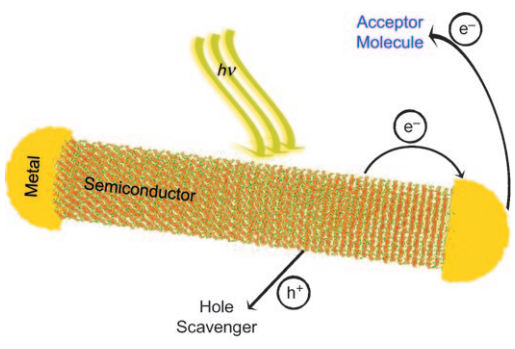

Figure 17. A photocatalytic redox reaction performed using a semiconductor–metal nanodumbbell. The semiconductor part absorbs a photon, forming an electron–hole pair. Charge separation occurs, with the electron transferring to the metal tip. The electrons from the metal reduce an acceptor molecule, while the holes from the semiconductor oxidize a hole-scavenging molecule. [From Ref. [176], copyright 2008 American Chemical Society.]

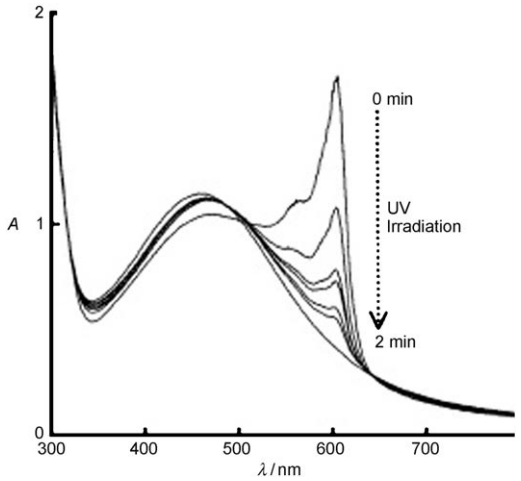

Figure 18. Absorption spectra of Ag@TiO_2 in the presence of thionine in deaerated ethanol following UV irradiation, demonstrating the reduction of the thionine (peak disappearance) as a function of irradiation time. [From Ref. [173], copyright 2004 American Chemical Society].

New highly controlled metal–semiconductor hybrid nanoparticles discussed herein also open up opportunities in designing a new family of photocatalytic materials. A limitation in previous nanoscale photocatlytic systems was that most studies focused on oxide semiconductors in which the absorption is only in the UV region, which consists of only about 4% of the entire solar spectrum. Clearly, efficient photocatalysts must have absorption that extends into the visible range. Furthermore, the high degree of control over the hybrid nanoparticles should allow for tailoring of the properties in terms of the band gap and band offsets necessary for the photocatlytic activity. First steps in this direction were reported in which photocatalytic activity was demonstrated for new metal–semiconductor hybrids. Photocatalytic reduction was studied on a model system, namely methylene blue dye molecules, under visible light irradiation with platinum and gold grown on CdSe nanorods.[103,176] The reduction of the dye molecules was followed using absorption spectroscopy, as the characteristic dye peaks diminished when the dye was reduced to leucomethylene blue by Pt/CdSe hybrids (Figure 19a). The photocatalytic efficiency is enhanced in the hybrid nanocrystal systems; the hybrid nanocrystals reduce significantly more dye molecules than either nanocrystal component by itself or a physical mixture of the components.[176] Moreover, the system maintained its photocatalytic

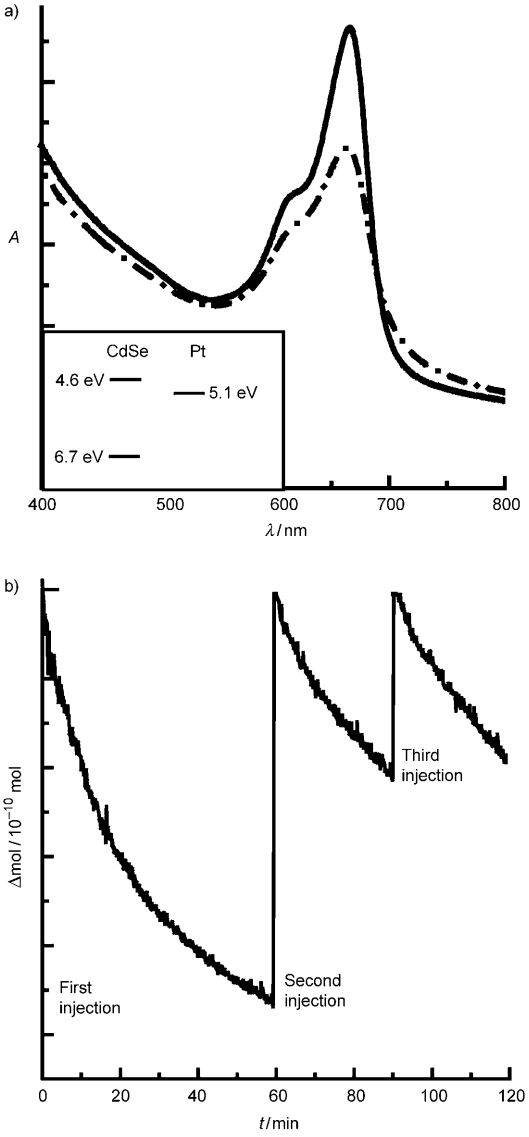

Figure 19. Photocatalysis of Pt/CdSe hybrid. a) Absorbance spectra of methylene blue (MB) and Pt/CdSe nanonets before (——) and after 60 min of irradiation (–•–•). The peak diminishes after irradiation. Inset: positions of the valence- and conduction-band levels below the vacuum level for 4 nm CdSe nanocrystals, and the Fermi level of platinum. b) Sequential photocatalysis experiment of the Pt/CdSe nanonet showing three injections of methylene blue at various times (the second and third are half batches) during irradiation of the nanonet sample. [From Ref. [103].]

activity upon further additions of dye, as can be seen in Figure 19b.

Charge retention could also be achieved for the hybrid nanoparticles by irradiating the deaerated solution in the presence of a hole acceptor, such as ethanol. After pre-irradiation, the number of stored electrons could be monitored by the reduction of methylene blue through the change in its absorbance. Interestingly, Au/CdSe nanodumbbels showed a high degree of charge retention under such a process, while the Pt/CdSe hybrids did not. This result is consistent with the tendency of gold to store electrons whereas platinum nanoparticles are known to release the charge.[147]

Perhaps the most challenging photocatalytic application is that of photochemical water splitting to form hydrogen and oxygen. This intriguing approach converts solar energy into chemical energy while the hydrogen can be used as a green fuel. Different studies have examined the use of hybrid metal–semiconductor nanoparticles to reroute solar energy to this reaction.[163,177–179] The aim of most studies is the use of visible light for this reaction, requiring efficient absorption in the visible range by the semiconductor. This goal might be realized by constructing nanohybrid z-scheme systems, which involves two-step photon excitation and charge separation,[180] and complex hybrid systems that allow good light absorbance and charge separation.[181,182] The efficiency and plausibility of these approaches deserves further study.

5. Summary and Outlook

This Review presents many of the diverse types of colloidal hybrid metal–semiconductor nanomaterials that have been synthesized over the last several years. While the range of material combinations, geometries, and properties that have been presented is impressive, this area of study within nanoscience still presents significant challenges for research before the goal of engineering nanomaterial properties is realized to its full potential. One challenge is to understand how growth conditions can be controlled to join two materials that may have very different structural and physical properties, and do so while controlling the final nanomaterial geometry. As more strategies for synthesizing hybrid nanomaterials are developed, a coherent picture of how reaction conditions and material combinations can be tuned to influence the growth mechanism of the hybrid material is yet to emerge. As these strategies become more robust, a diverse library of material combinations, arranged in different geometries, will provide insight into the interaction of different material systems at the nanometer scale.

At the very least, such material combinations should lead to multifunctional hybrid particles, such as luminescence biolabels or catalytic particles, which may be recovered easily using magnetic fields. Contact points on the hybrids may allow further development of bottom-up assembly strategies for constructing complex electrical and optical devices. Judicious combinations of materials may lead to hybrid nanomaterials with new properties that could be applicable to solar energy harvesting. Applications in other fields, such as spintronics or smart sensors, need to be demonstrated upon development of suitable hybrid nanoparticles. Although such explorations are still in an early stage, the ability to tune the properties or impart multiple functionalities to hybrid nanomaterials shows high potential for their future inclusion in emerging technologies.

U.B. acknowledges funding of the Israel Science Foundation (grant 972/08) and the Alfred and Erica Larisch Memorial Chair in Solar Energy. R.C. thanks the CAMBR foundation for a graduate student fellowship. A.E.S. acknowledges fund-

ing from the U.S. National Science Foundation (OISE-0601919). We are indebted to our colleagues who have contributed to scientific work on hybrid nanoaparticles in our group: Asaf Salant, Taleb Mokari, Einat Elmalem, Dirk Dorfs, and Gabi Menagen, and to our colleagues: Oded Millo, Dov Steiner, Eran Rabani, Guy Cohen, and Katerina Soulantica. We thank our group member Amit Sitt for the design of the cover image.

Received: October 26, 2009
Published online: June 11, 2010

[1] A. P. Alivisatos, *Science* **1996**, *271*, 933.
[2] C. B. Murray, C. R. Kagan, M. G. Bawendi, *Annu. Rev. Mater. Sci.* **2000**, *30*, 545.
[3] A. L. Efros, M. Rosen, *Annu. Rev. Mater. Sci.* **2000**, *30*, 475.
[4] U. Banin, O. Millo, *Annu. Rev. Phys. Chem.* **2003**, *54*, 465.
[5] X. Peng, U. Manna, W. Yang, J. Wickham, E. Scher, A. Kadavanich, A. P. Alivisatos, *Nature* **2000**, *404*, 59.
[6] S. Kan, T. Mokari, E. Rothenberg, U. Banin, *Nat. Mater.* **2003**, *2*, 155.
[7] C. J. Murphy, A. M. Gole, S. E. Hunyadi, J. W. Stone, P. N. Sisco, A. Alkilany, B. E. Kinard, P. Hankins, *Chem. Commun.* **2008**, 544.
[8] A. R. Tao, S. Habas, P. D. Yang, *Small* **2008**, *4*, 310.
[9] L. Li, T. J. Daou, I. Texier, T. K. C. Tran, Q. L. Nguyen, P. Reiss, *Chem. Mater.* **2009**, *21*, 2422.
[10] M. L. Schipper, G. Iyer, A. L. Koh, Z. Cheng, Y. Ebenstein, A. Aharoni, S. Keren, L. A. Bentolila, J. Q. Li, J. H. Rao, X. Y. Chen, U. Banin, A. M. Wu, R. Sinclair, S. Weiss, S. S. Gambhir, *Small* **2009**, *5*, 126.
[11] C. G. Hacliipanayis, M. J. Bonder, S. Balakrishanan, X. Wang, H. Mao, G. C. Hadjipanayis, *Small* **2008**, *4*, 1925.
[12] J. R. Cole, N. A. Mirin, M. W. Knight, G. P. Goodrich, N. J. Halas, *J. Phys. Chem. C* **2009**, *113*, 12090.
[13] A. V. Malko, A. A. Mikhailovsky, M. A. Petruska, J. A. Hollingsworth, H. Htoon, M. G. Bawendi, V. I. Klimov, *Appl. Phys. Lett.* **2002**, *81*, 1303.
[14] V. Medvedev, M. Kazes, S. Kan, U. Banin, Y. Talmon, N. Tessler, *Synth. Met.* **2003**, *137*, 1047.
[15] M. Kazes, D. Y. Lewis, U. Banin, *Adv. Funct. Mater.* **2004**, *14*, 957.
[16] I. Gur, N. A. Fromer, M. L. Geier, A. P. Alivisatos, *Science* **2005**, *310*, 462.
[17] J. H. Bang, P. V. Kamat, *Acs Nano* **2009**, *3*, 1467.
[18] D. V. Talapin, C. B. Murray, *Science* **2005**, *310*, 86.
[19] T. Mokari, E. Rothenberg, I. Popov, R. Costi, U. Banin, *Science* **2004**, *304*, 1787.
[20] A. E. Saunders, I. Popov, U. Banin, *J. Phys. Chem. B* **2006**, *110*, 25421.
[21] W. L. Shi, H. Zeng, Y. Sahoo, T. Y. Ohulchanskyy, Y. Ding, Z. L. Wang, M. Swihart, P. N. Prasad, *Nano Lett.* **2006**, *6*, 875.
[22] H. W. Gu, R. K. Zheng, X. X. Zhang, B. Xu, *J. Am. Chem. Soc.* **2004**, *126*, 5664.
[23] H. Yu, M. Chen, P. M. Rice, S. X. Wang, R. L. White, S. H. Sun, *Nano Lett.* **2005**, *5*, 379.
[24] H. Kim, M. Achermann, L. P. Balet, J. A. Hollingsworth, V. I. Klimov, *J. Am. Chem. Soc.* **2005**, *127*, 544.
[25] R. Buonsanti, V. Grillo, E. Carlino, C. Giannini, M. L. Curri, C. Innocenti, C. Sangregorio, K. Achterhold, F. G. Parak, A. Agostiano, P. D. Cozzoli, *J. Am. Chem. Soc.* **2006**, *128*, 16953.
[26] D. V. Talapin, H. Yu, E. V. Shevchenko, A. Lobo, C. B. Murray, *J. Phys. Chem. C* **2007**, *111*, 14049.
[27] B. H. Juárez, C. Klinke, A. Kornowski, H. Weller, *Nano Lett.* **2007**, *7*, 3564.
[28] J. H. Gao, G. L. Liang, J. S. Cheung, Y. Pan, Y. Kuang, F. Zhao, B. Zhang, X. X. Zhang, E. X. Wu, B. Xu, *J. Am. Chem. Soc.* **2008**, *130*, 11828.
[29] E. V. Shevchenko, M. I. Bodnarchitk, M. V. Kovalenko, D. V. Talapin, R. K. Smith, S. Aloni, W. Heiss, A. P. Alivisatos, *Adv. Mater.* **2008**, *20*, 4323.
[30] Z. H. Sun, Z. Yang, J. H. Zhou, M. H. Yeung, W. H. Ni, H. K. Wu, J. F. Wang, *Angew. Chem.* **2009**, *121*, 2925; *Angew. Chem. Int. Ed.* **2009**, *48*, 2881.
[31] L. Manna, J. Milliron Delia, A. Meisel, C. Scher Erik, A. P. Alivisatos, *Nat. Mater.* **2003**, *2*, 382.
[32] W. W. Yu, Y. A. Wang, X. Peng, *Chem. Mater.* **2003**, *15*, 4300.
[33] Y. Yin, A. P. Alivisatos, *Nature* **2005**, *437*, 664.
[34] F. Shieh, A. E. Saunders, B. A. Korgel, *J. Phys. Chem. B* **2005**, *109*, 8538.
[35] H. Yu, P. C. Gibbons, K. F. Kelton, W. E. Buhro, *J. Am. Chem. Soc.* **2001**, *123*, 9198.
[36] T. Hanrath, B. A. Korgel, *Adv. Mater.* **2003**, *15*, 437.
[37] A. Gole, C. J. Murphy, *Chem. Mater.* **2004**, *16*, 3633.
[38] K. T. Yong, Y. Sahoo, K. R. Choudhury, M. T. Swihart, J. R. Minter, P. N. Prasad, *Nano Lett.* **2006**, *6*, 709.
[39] L. Carbone, C. Nobile, M. De Giorg, F. D. Sala, G. Morello, P. Pompa, M. Hytch, E. Snoeck, A. Fiore, I. R. Franchini, M. Nadasan, A. F. Silvestre, L. Chiodo, S. Kudera, R. Cingolani, R. Krahne, L. Manna, *Nano Lett.* **2007**, *7*, 2942.
[40] Z. Y. Tang, N. A. Kotov, M. Giersig, *Science* **2002**, *297*, 237.
[41] W. G. Lu, P. X. Gao, W. Bin Jian, Z. L. Wang, J. Y. Fang, *J. Am. Chem. Soc.* **2004**, *126*, 14816.
[42] K. S. Cho, D. V. Talapin, W. Gaschler, C. B. Murray, *J. Am. Chem. Soc.* **2005**, *127*, 7140.
[43] Y. W. Jun, Y. Y. Jung, J. Cheon, *J. Am. Chem. Soc.* **2002**, *124*, 615.
[44] L. Manna, E. C. Scher, A. P. Alivisatos, *J. Cluster Sci.* **2002**, *13*, 521.
[45] M. J. Bierman, Y. K. A. Lau, A. V. Kvit, A. L. Schmitt, S. Jin, *Science* **2008**, *320*, 1060.
[46] W. X. Niu, Z. Y. Li, L. H. Shi, X. Q. Liu, H. J. Li, S. Han, J. Chen, G. B. Xu, *Cryst. Growth Des.* **2008**, *8*, 4440.
[47] Y. H. Wei, R. Klajn, A. O. Pinchuk, B. A. Grzybowski, *Small* **2008**, *4*, 1635.
[48] M. Grzelczak, J. Perez-Juste, P. Mulvaney, L. M. Liz-Marzan, *Chem. Soc. Rev.* **2008**, *37*, 1783.
[49] G. Kawamura, Y. Yang, K. Fukuda, M. Nogami, *Mater. Chem. Phys.* **2009**, *115*, 229.
[50] B. Altansukh, J. X. Yao, D. Wang, *J. Nanosci. Nanotechnol.* **2009**, *9*, 1300.
[51] A. Henglein, *Chem. Rev.* **1989**, *89*, 1861.
[52] M. L. Steigerwald, L. E. Brus, *Acc. Chem. Res.* **1990**, *23*, 183.
[53] C. B. Murray, D. J. Norris, M. G. Bawendi, *J. Am. Chem. Soc.* **1993**, *115*, 8706.
[54] M. Brust, M. Walker, D. Bethell, D. J. Schiffrin, R. Whyman, *J. Chem. Soc. Chem. Commun.* **1994**, 801.
[55] J. Park, J. Joo, S. G. Kwon, Y. Jang, T. Hyeon, *Angew. Chem.* **2007**, *119*, 4714; *Angew. Chem. Int. Ed.* **2007**, *46*, 4630.
[56] C. Pacholski, A. Kornowski, H. Weller, *Angew. Chem.* **2002**, *114*, 1234; *Angew. Chem. Int. Ed.* **2002**, *41*, 1188.
[57] W. E. Buhro, V. L. Colvin, *Nat. Mater.* **2003**, *2*, 138.
[58] C. J. Barrelet, Y. Wu, D. C. Bell, C. M. Lieber, *J. Am. Chem. Soc.* **2003**, *125*, 11498.
[59] C. J. Murphy, T. K. San, A. M. Gole, C. J. Orendorff, J. X. Gao, L. Gou, S. E. Hunyadi, T. Li, *J. Phys. Chem. B* **2005**, *109*, 13857.
[60] T. S. Ahmadi, Z. L. Wang, T. C. Green, A. Henglein, M. A. ElSayed, *Science* **1996**, *272*, 1924.
[61] Z. L. Wang, T. S. Ahmad, M. A. ElSayed, *Surf. Sci.* **1997**, *380*, 302.
[62] M. A. ElSayed, T. Ahmadi, J. Petrowski, *Abst. Pap. Am. Chem. Soc.* **1997**, *213*, 306.

[63] L. E. Brus, *J. Chem. Phys.* **1984**, *80*, 4403.
[64] D. V. Averin, K. K. Likharev, *Mesoscopic Phenomena in Solids*, Elsevier, Amstredam, **1991**.
[65] M. H. Devoret, H. Grabert, *Single Charge Tunneling: Coulomb Blockade Phenomena in Nanostructures*, Vol. *294*, Pleum, New York, **1992**.
[66] U. Banin, Y. W. Cao, D. Katz, O. Millo, *Nature* **1999**, *400*, 542.
[67] L. M. Liz-Marzan, *Mater. Today* **2004**, *7*, 26.
[68] J. T. Hu, L. S. Li, W. D. Yang, L. Manna, L. W. Wang, A. P. Alivisatos, *Science* **2001**, *292*, 2060.
[69] E. Rothenberg, Y. Ebenstein, M. Kazes, U. Banin, *J. Phys. Chem. B* **2004**, *108*, 2797.
[70] G. C. Papavassiliou, *Prog. Solid State Chem.* **1979**, *12*, 185.
[71] B. M. I. vanderZande, M. R. Bohmer, L. G. J. Fokkink, C. Schonenberger, *J. Phys. Chem. B* **1997**, *101*, 852.
[72] M. B. Mohamed, K. Z. Ismail, S. Link, M. A. El-Sayed, *J. Phys. Chem. B* **1998**, *102*, 9370.
[73] V. M. Cepak, C. R. Martin, *J. Phys. Chem. B* **1998**, *102*, 9985.
[74] A. Mews, A. Eychmuller, M. Giersig, D. Schooss, H. Weller, *J. Phys. Chem.* **1994**, *98*, 934.
[75] B. O. Dabbousi, J. RodriguezViejo, F. V. Mikulec, J. R. Heine, H. Mattoussi, R. Ober, K. F. Jensen, M. G. Bawendi, *J. Phys. Chem. B* **1997**, *101*, 9463.
[76] X. G. Peng, M. C. Schlamp, A. V. Kadavanich, A. P. Alivisatos, *J. Am. Chem. Soc.* **1997**, *119*, 7019.
[77] S. A. Ivanov, J. Nanda, A. Piryatinski, M. Achermann, L. P. Balet, I. V. Bezel, P. O. Anikeeva, S. Tretiak, V. I. Klimov, *J. Phys. Chem. B* **2004**, *108*, 10625.
[78] K. Yu, B. Zaman, S. Romanova, D. S. Wang, J. A. Ripmeester, *Small* **2005**, *1*, 332.
[79] D. Oron, M. Kazes, U. Banin, *Phys. Rev. B* **2007**, *75*, 035330.
[80] S. Kumar, M. Jones, S. S. Lo, G. D. Scholes, *Small* **2007**, *3*, 1633.
[81] A. E. Saunders, B. Koo, X. Wang, C. K. Shih, B. A. Korgel, *ChemPhysChem* **2008**, *9*, 1158.
[82] S. E. Habas, H. Lee, V. Radmilovic, G. A. Somorjai, P. Yang, *Nat. Mater.* **2007**, *6*, 692.
[83] T. Wetz, K. Soulantica, A. Talqui, M. Respaud, E. Snoeck, B. Chaudret, *Angew. Chem.* **2007**, *119*, 7209; *Angew. Chem. Int. Ed.* **2007**, *46*, 7079.
[84] C. L. Bracey, P. R. Ellis, G. J. Hutchings, *Chem. Soc. Rev.* **2009**, *38*, 2231.
[85] W. J. M. Mulder, R. Koole, R. J. Brandwijk, G. Storm, P. T. K. Chin, G. J. Strijkers, C. D. Donega, K. Nicolay, A. W. Griffioen, *Nano Lett.* **2006**, *6*, 1.
[86] B. P. Barnett, A. Arepally, P. V. Karmarkar, D. Qian, W. D. Gilson, P. Walczak, V. Howland, L. Lawler, C. Lauzon, M. Stuber, D. L. Kraitchman, J. W. M. Bulte, *Nat. Med.* **2007**, *13*, 986.
[87] A. Zaban, O. I. Micic, B. A. Gregg, A. J. Nozik, *Langmuir* **1998**, *14*, 3153.
[88] P. R. Yu, K. Zhu, A. G. Norman, S. Ferrere, A. J. Frank, A. J. Nozik, *J. Phys. Chem. B* **2006**, *110*, 25451.
[89] A. Sanchez, S. Abbet, U. Heiz, W. D. Schneider, H. Hakkinen, R. N. Barnett, U. Landman, *J. Phys. Chem. A* **1999**, *103*, 9573.
[90] M. S. Chen, D. W. Goodman, *Acc. Chem. Res.* **2006**, *39*, 739.
[91] P. D. Cozzoli, T. Pellegrino, L. Manna, *Chem. Soc. Rev.* **2006**, *35*, 1195.
[92] D. V. Leff, P. C. Ohara, J. R. Heath, W. M. Gelbart, *J. Phys. Chem.* **1995**, *99*, 7036.
[93] X. Peng, J. Wickham, A. P. Alivisatos, *J. Am. Chem. Soc.* **1998**, *120*, 5343.
[94] D. V. Talapin, A. L. Rogach, M. Haase, H. Weller, *J. Phys. Chem. B* **2001**, *105*, 12278.
[95] T. Mokari, C. G. Sztrum, A. Salant, E. Rabani, U. Banin, *Nat. Mater.* **2005**, *4*, 855.
[96] G. Menagen, D. Mocatta, A. Salant, I. Popov, D. Dorfs, U. Banin, *Chem. Mater.* **2008**, *20*, 6900.
[97] J. McBride, J. Treadway, L. C. Feldman, S. J. Pennycook, S. J. Rosenthal, *Nano Lett.* **2006**, *6*, 1496.
[98] J. Y. Rempel, B. L. Trout, M. G. Bawendi, K. F. Jensen, *J. Phys. Chem. B* **2006**, *110*, 18007.
[99] Z. A. Peng, X. G. Peng, *J. Am. Chem. Soc.* **2001**, *123*, 1389.
[100] A. Puzder, A. J. Williamson, N. Zaitseva, G. Galli, L. Manna, A. P. Alivisatos, *Nano Lett.* **2004**, *4*, 2361.
[101] J. Yang, H. I. Elim, Q. Zhang, J. Y. Lee, W. Ji, *J. Am. Chem. Soc.* **2006**, *128*, 11921.
[102] J. Yang, L. Levina, E. H. Sargent, S. O. Kelley, *J. Mater. Chem.* **2006**, *16*, 4025.
[103] E. Elmalem, A. E. Saunders, R. Costi, A. Salant, U. Banin, *Adv. Mater.* **2008**, *20*, 4312.
[104] M. Casavola, V. Grillo, E. Carlino, C. Giannini, F. Gozzo, E. F. Pinel, M. A. Garcia, L. Manna, R. Cingolani, P. D. Cozzoli, *Nano Lett.* **2007**, *7*, 1386.
[105] S. E. Habas, P. D. Yang, T. Mokari, *J. Am. Chem. Soc.* **2008**, *130*, 3294.
[106] C. Pacholski, A. Kornowski, H. Weller, *Angew. Chem.* **2004**, *116*, 4878; *Angew. Chem. Int. Ed.* **2004**, *43*, 4774.
[107] G. Dukovic, M. G. Merkle, J. H. Nelson, S. M. Hughes, A. P. Alivisatos, *Adv. Mater.* **2008**, *20*, 4306.
[108] L. Carbone, A. Jakab, Y. Khalavka, C. Sönnichsen, *Nano Lett.* **2009**, *9*, 3710.
[109] G. Menagen, J. E. Macdonald, Y. Shemesh, I. Popov, U. Banin, *J. Am. Chem. Soc.* **2009**, *131*, 17406.
[110] T. Mokari, A. Aharoni, I. Popov, U. Banin, *Angew. Chem.* **2006**, *118*, 8169; *Angew. Chem. Int. Ed.* **2006**, *45*, 8001.
[111] Y. D. Yin, R. M. Rioux, C. K. Erdonmez, S. Hughes, G. A. Somorjai, A. P. Alivisatos, *Science* **2004**, *304*, 711.
[112] A. Cabot, M. Ibanez, P. Guardia, A. P. Alivisatos, *J. Am. Chem. Soc.* **2009**, *131*, 11326.
[113] J. H. Gao, B. Zhang, Y. Gao, Y. Pan, X. X. Zhang, B. Xu, *J. Am. Chem. Soc.* **2007**, *129*, 11928.
[114] A. E. Saunders, I. Popov, U. Banin, *Z. Anorg. Allg. Chem.* **2007**, *633*, 2414.
[115] M. Z. Liu, P. Guyot-Sionnest, *J. Mater. Chem.* **2006**, *16*, 3942.
[116] L. Carbone, S. Kudera, C. Giannini, G. Ciccarella, R. Cingolani, P. D. Cozzoli, L. Manna, *J. Mater. Chem.* **2006**, *16*, 3952.
[117] Y. Khalavka, C. Sönnichsen, *Adv. Mater.* **2008**, *20*, 588.
[118] J. Lee, A. O. Govorov, J. Dulka, N. A. Kotov, *Nano Lett.* **2004**, *4*, 2323.
[119] J. Lee, T. Javed, T. Skeini, A. O. Govorov, G. W. Bryant, N. A. Kotov, *Angew. Chem.* **2006**, *118*, 4937; *Angew. Chem. Int. Ed.* **2006**, *45*, 4819.
[120] A. O. Govorov, G. W. Bryant, W. Zhang, T. Skeini, J. Lee, N. A. Kotov, J. M. Slocik, R. R. Naik, *Nano Lett.* **2006**, *6*, 984.
[121] F. X. Redl, K. S. Cho, C. B. Murray, S. O'Brien, *Nature* **2003**, *423*, 968.
[122] A. E. Saunders, B. A. Korgel, *ChemPhysChem* **2005**, *6*, 61.
[123] E. V. Shevchenko, D. V. Talapin, S. O'Brien, C. B. Murray, *J. Am. Chem. Soc.* **2005**, *127*, 8741.
[124] E. V. Shevchenko, D. V. Talapin, C. B. Murray, S. O'Brien, *J. Am. Chem. Soc.* **2006**, *128*, 3620.
[125] E. V. Shevchenko, D. V. Talapin, N. A. Kotov, S. O'Brien, C. B. Murray, *Nature* **2006**, *439*, 55.
[126] J. Cheon, J. I. Park, J. S. Choi, Y. W. Jun, S. Kim, M. G. Kim, Y. M. Kim, Y. J. Kim, *Proc. Natl. Acad. Sci. USA* **2006**, *103*, 3023.
[127] W. G. Lu, J. Y. Fang, J. Lin, J. Zhang, Z. Y. Sun, K. L. Stokes, *J. Nanosci. Nanotechnol.* **2006**, *6*, 1662.
[128] Z. Y. Chen, J. Moore, G. Radtke, H. Sirringhaus, S. O'Brien, *J. Am. Chem. Soc.* **2007**, *129*, 15702.
[129] J. J. Urban, D. V. Talapin, E. V. Shevchenko, C. R. Kagan, C. B. Murray, *Nat. Mater.* **2007**, *6*, 115.
[130] C. Lu, Z. Chen, S. O'Brien, *Chem. Mater.* **2008**, *20*, 3594.

[131] E. V. Shevchenko, M. Ringler, A. Schwemer, D. V. Talapin, T. A. Klar, A. L. Rogach, J. Feldmann, A. P. Alivisatos, *J. Am. Chem. Soc.* **2008**, *130*, 3274.
[132] Y. W. Cao, U. Banin, *J. Am. Chem. Soc.* **2000**, *122*, 9692.
[133] L. Manna, E. C. Scher, L. S. Li, A. P. Alivisatos, *J. Am. Chem. Soc.* **2002**, *124*, 7136.
[134] J. J. Li, Y. A. Wang, W. Z. Guo, J. C. Keay, T. D. Mishima, M. B. Johnson, X. G. Peng, *J. Am. Chem. Soc.* **2003**, *125*, 12567.
[135] A. Mews, A. V. Kadavanich, U. Banin, A. P. Alivisatos, *Phys. Rev. B* **1996**, *53*, R13242.
[136] R. B. Little, M. A. El-Sayed, G. W. Bryant, S. Burke, *J. Chem. Phys.* **2001**, *114*, 1813.
[137] K. W. Kwon, M. Shim, *J. Am. Chem. Soc.* **2005**, *127*, 10269.
[138] E. Yoskovitz, D. Oron, I. Shweky, U. Banin, *J. Phys. Chem. C* **2008**, *112*, 16306.
[139] Y. Chen, K. Munechika, D. S. Ginger, *Nano Lett.* **2007**, *7*, 690.
[140] K. T. Yong, Y. Sahoo, K. R. Choudhury, M. T. Swihart, J. R. Minter, P. N. Prasad, *Chem. Mater.* **2006**, *18*, 5965.
[141] H. Y. Lin, Y. F. Chen, J. G. Wu, D. I. Wang, C. C. Chen, *Appl. Phys. Lett.* **2006**, *88*, 161911.
[142] P. Mulvaney, *Langmuir* **1996**, *12*, 788.
[143] A. Many, Y. Goldstein, N. B. Grover, *Semiconductor Surfaces*, North Holland, Amsterdam, **1965**.
[144] U. Landman, R. N. Barnett, A. G. Scherbakov, P. Avouris, *Phys. Rev. Lett.* **2000**, *85*, 1958.
[145] D. Steiner, T. Mokari, U. Banin, O. Millo, *Phys. Rev. Lett.* **2005**, *95*, 056805.
[146] D. Katz, T. Wizansky, O. Millo, E. Rothenberg, T. Mokari, U. Banin, *Phys. Rev. Lett.* **2002**, *89*, 086801.
[147] A. Wood, M. Giersig, P. Mulvaney, *J. Phys. Chem. B* **2001**, *105*, 8810.
[148] R. Costi, G. Cohen, A. Salant, E. Rabani, U. Banin, *Nano Lett.* **2009**, *9*, 2031.
[149] O. Cherniavskaya, L. W. Chen, V. Weng, L. Yuditsky, L. E. Brus, *J. Phys. Chem. B* **2003**, *107*, 1525.
[150] T. D. Krauss, L. E. Brus, *Mater. Sci. Eng. B* **2000**, *69*, 289.
[151] J. Maynadié, A. Salant, A. Falqui, M. Respaud, E. Shaviv, U. Banin, K. Soulantica, B. Chaudret, *Angew. Chem.* **2009**, *121*, 1846; *Angew. Chem. Int. Ed.* **2009**, *48*, 1814.
[152] Y. Cui, U. Banin, M. T. Bjork, A. P. Alivisatos, *Nano Lett.* **2005**, *5*, 1519.
[153] Y. Cui, U. Banin, G. Ram, A. P. Alivisatos, *Abst. Pap. Am. Chem. Soc.* **2005**, *229*, 409.
[154] M. T. Sheldon, P. E. Trudeau, T. Mokari, L. W. Wang, A. P. Alivisatos, *Nano Lett.* **2009**, *9*, 3676.
[155] A. Salant, E. Amitay-Sadovsky, U. Banin, *J. Am. Chem. Soc.* **2006**, *128*, 10006.
[156] A. Figuerola, I. R. Franchini, A. Fiore, R. Mastria, A. Falqui, G. Bertoni, S. Bals, G. Van Tendeloo, S. Kudera, R. Cingolani, L. Manna, *Adv. Mater.* **2009**, *21*, 550.
[157] N. Zhao, K. Liu, J. Greener, Z. H. Nie, E. Kumacheva, *Nano Lett.* **2009**, *9*, 3077.
[158] S. Ahmed, K. M. Ryan, *Nano Lett.* **2007**, *7*, 2480.
[159] S. T. Selvan, P. K. Patra, C. Y. Ang, J. Y. Ying, *Angew. Chem.* **2007**, *119*, 2500; *Angew. Chem. Int. Ed.* **2007**, *46*, 2448.
[160] N. Pazos-Peréz, Y. Gao, M. Hilgendorff, S. Irsen, J. Perez-Juste, M. Spasova, M. Farle, L. M. Liz-Marzan, M. Giersig, *Chem. Mater.* **2007**, *19*, 4415.
[161] A. Mills, R. H. Davies, D. Worsley, *Chem. Soc. Rev.* **1993**, *22*, 417.
[162] K. Sunada, Y. Kikuchi, K. Hashimoto, A. Fujishima, *Environ. Sci. Technol.* **1998**, *32*, 726.
[163] M. Grätzel, *Nature* **2001**, *414*, 338.
[164] A. Fujishima, K. Honda, *Nature* **1972**, *238*, 37.
[165] A. J. Bard, M. A. Fox, *Acc. Chem. Res.* **1995**, *28*, 141.
[166] N. S. Lewis, D. G. Nocera, *Proc. Natl. Acad. Sci. USA* **2006**, *103*, 15729.
[167] N. S. Lewis, *Science* **2007**, *315*, 798.
[168] N. Bao, L. Shen, T. Takata, K. Domen, *Chem. Mater.* **2008**, *20*, 110.
[169] R. Narayanan, M. A. El-Sayed, *Nano Lett.* **2004**, *4*, 1343.
[170] C. A. Stowell, B. A. Korgel, *Nano Lett.* **2005**, *5*, 1203.
[171] J. Park, E. Kang, S. U. Son, H. M. Park, M. K. Lee, J. Kim, K. W. Kim, H. J. Noh, J. H. Park, C. J. Bae, J. G. Park, T. Hyeon, *Adv. Mater.* **2005**, *17*, 429.
[172] N. Tian, Z. Y. Zhou, S. G. Sun, Y. Ding, Z. L. Wang, *Science* **2007**, *316*, 732.
[173] T. Hirakawa, P. V. Kamat, *Langmuir* **2004**, *20*, 5645.
[174] T. Hirakawa, P. V. Kamat, *J. Am. Chem. Soc.* **2005**, *127*, 3928.
[175] P. K. Sudeep, K. Takechi, P. V. Kamat, *J. Phys. Chem. C* **2007**, *111*, 488.
[176] R. Costi, A. E. Saunders, E. Elmalem, A. Salant, U. Banin, *Nano Lett.* **2008**, *8*, 637.
[177] J. H. Park, O. O. Park, S. Kim, *Appl. Phys. Lett.* **2006**, *89*, 163106.
[178] K. Maeda, K. Domen, *J. Phys. Chem. C* **2007**, *111*, 7851.
[179] M. A. Khan, O. B. Yang, *Catal. Today* **2009**, *146*, 177.
[180] H. Tada, T. Mitsui, T. Kiyonaga, T. Akita, K. Tanaka, *Nat. Mater.* **2006**, *5*, 782.
[181] H. Park, W. Choi, M. R. Hoffmann, *J. Mater. Chem.* **2008**, *18*, 2379.
[182] J. S. Jang, S. H. Choi, H. G. Kim, J. S. Lee, *J. Phys. Chem. C* **2008**, *112*, 17200.